Diffusive Molecular Dynamics for Mass Transport Applications

Michael Ortiz
California Institute of Technology and
Rheinische Friedrich-Wilhelms Universität Bonn

Collaborators: M.P. Ariza (Seville), J.P. Mendez (Caltech), X. Sun (Caltech), M. Ponga (UBC), K.G. Wang (VPI&SU), I.G. Ringdalen (SINTEF), Z. Zhang (NTNU)

Max-Planck-Institut für Eisenforschung GmbH
40237 Düsseldorf, Germany
December 14, 2018

Motivation – Diffusive time scale

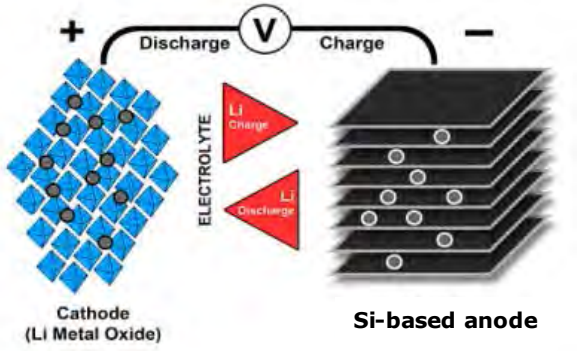

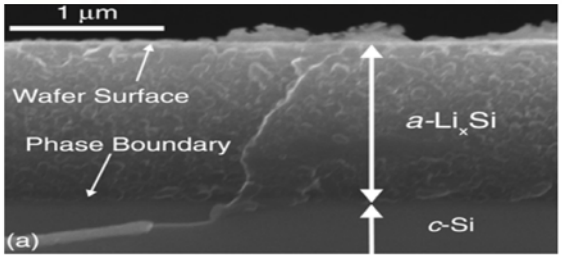

M. J. Chon *et al.*, *Phys. Rev. Lett.*, **107** (2011) 045503.

- Si-based anodes in Li-ion batteries
- Silicon loses crystalline structure upon lithiation and amorphizes
- Volume increase of 300%
- Loss of structure integrity and function after a few charge cycles

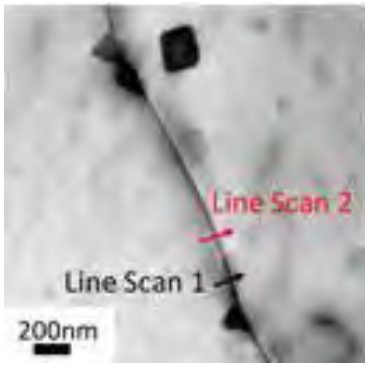

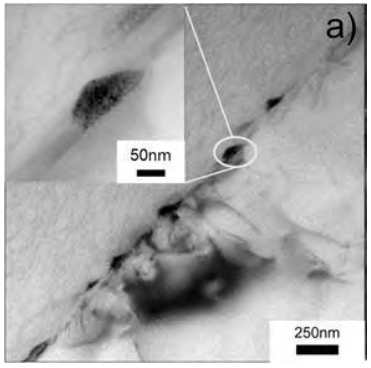

R. Zhang *et al.*, *Scientific Reports*, **7** (2017) 2961.

- Al-Mg 5xxxx series alloys
- Sensitization due to GBs
- Formation of β phase (Mg_2Al_3)
- Stress corrosion cracking

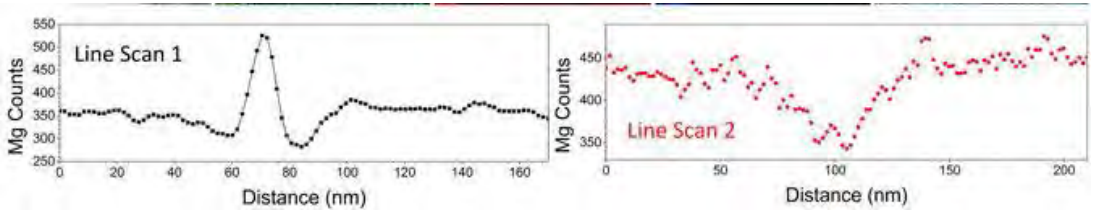

Michael Ortiz
MPIE 2018

The spatial and temporal gaps

- The essential difficulty: *Multiple scales*
  - *Atomic level rate-limiting processes: Thermal activation, transport, defects, grain boundaries…*
  - *But macroscopic processes of interest:*
    - *Microstructure evolution in alloys*
    - *Long-term transport phenomena: Heat, mass…*
    - *Full chemistry: Corrosion, combustion…*
- *Time-scale gap*: From molecular dynamics (femtosecond) to macroscopic (seconds-years)
- *Spatial-scale gap*: From lattice defects (Angstroms) to macroscopic (mm-m)
- Problem intractable by brute force (even with exascale computing ☺), *ergo* must think…

Diffusive Molecular Dynamics (DMD)

- *Objectives*: Thermodynamics without all the thermal vibrations; mass transport without all the hops; atomistics without all the atoms…
- Our approach[1,2] (max-ent+kinetics+QC):
  - *Treat atomic-level fluctuations statistically (away from equilibrium) through **maximum-entropy principle***
  - *Append Onsager-like **empirical atomic-level kinetic laws** (heat and mass transport)*
  - *Quasicontinuum spatial coarse-graining*
- Implementation:
  - *Meanfield approximation of phase integrals*
  - *Quasistatic, forward integration of transport equations*

[1]Y. Kulkarni, J. Knap & MO, *J. Mech. Phys. Solids*, **56** (2008) 1417.

[2]G. Venturini, K. Wang, I. Romero, M.P. Ariza & MO, *J. Mech. Phys. Solids*, **73** (2014) 242-268.

Max-Ent Non-Equilibrium SM

- Grand-canonical ensemble, N atoms, M species:
  - State: $(\{\boldsymbol{q}\}, \{\boldsymbol{p}\}, \{\boldsymbol{n}\}) \in \mathbb{R}^{3N} \times \mathbb{R}^{3N} \times \mathcal{O}_{NM}$
  - Atomic positions: $\{\boldsymbol{q}\} = \{\boldsymbol{q}_1, \ldots, \boldsymbol{q}_N\}$
  - Atomic momenta: $\{\boldsymbol{p}\} = \{\boldsymbol{p}_1, \ldots, \boldsymbol{p}_N\}$
  - Occupancy: $n_{ik} = \begin{cases} 1, & \text{site } i \text{ occupied by species } k, \\ 0, & \text{otherwise.} \end{cases}$

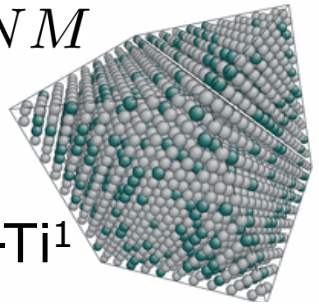
Al-Ti[1]

- Ensemble average of observable: $\langle A \rangle =$

$$\sum_{\{\boldsymbol{n}\} \in \mathcal{O}_{NM}} \int A(\{\boldsymbol{q}\}, \{\boldsymbol{p}\}, \{\boldsymbol{n}\})\, \rho(\{\boldsymbol{q}\}, \{\boldsymbol{p}\}, \{\boldsymbol{n}\})\, dq\, dp$$

↑ grand-canonical pdf

J. von Pezold, A. Dick, M. Friak and J. Negebauer, Phys. Rev. B, 81 (2010) 094203.

Max-Ent Non-Equilibrium SM

- Assume $H = \sum_{i=1}^{N} h_i$, (e. g., EAM, TB...)
- Principle of max-ent[1]: $\mathcal{S}[p] = -k_B \langle \log \rho \rangle \rightarrow \max!$

  subject to: $\left.\begin{aligned} \langle \boldsymbol{q}_i \rangle = \bar{\boldsymbol{q}}_i, \;\; \langle \boldsymbol{p}_i \rangle = \bar{\boldsymbol{p}}_i, \\ \langle h_i \rangle = e_i, \;\; \langle n_{ik} \rangle = x_{ik} \end{aligned}\right\}$ local constraints!

- Lagrangian: reciprocal temperatures ↓ β, chemical potentials ↓ γ

$$\mathcal{L}[p, \{\beta\}, \{\gamma\}] = \mathcal{S}[p] - k_B \{\beta\}^T \{\langle h \rangle\} - k_B \{\gamma\}^T \{\langle \boldsymbol{n} \rangle\}$$

- Gran-canonical pdf: $\rho = \frac{1}{\Xi} \mathrm{e}^{-\{\beta\}^T \{h\} - \{\gamma\}^T \{\boldsymbol{n}\}},$

on affine subspace $\left\{ \langle \{\boldsymbol{q}\} \rangle = \{\bar{\boldsymbol{q}}\}, \langle \{\boldsymbol{p}\} \rangle = \{\bar{\boldsymbol{p}}\} \right\}$

[1]E.T. Jaynes, *Physical Review Series* II, **106**(4) (1957) 620–630; **108**(2) (1957) 171–190.

Max-Ent Non-Equilibrium SM

- Gran-canonical free entropy:

$$\Phi(\{\bar{\boldsymbol{q}}\},\{\bar{\boldsymbol{p}}\},\{\beta\},\{\gamma\}) = k_B \log \Xi$$

- Local equilibrium relations:

$$e_i = -\frac{1}{k_B}\frac{\partial \Phi}{\partial \beta_i}, \quad x_{ik} = \frac{1}{k_B}\frac{\partial \Phi}{\partial \gamma_{ik}}$$

- Mesoscopic dynamics: quasistatic!

$$\beta_i \frac{d\bar{\boldsymbol{q}}_i}{dt} = \frac{1}{k_B}\frac{\partial \Phi}{\partial \bar{\boldsymbol{p}}_i}, \quad \beta_i \frac{d\bar{\boldsymbol{p}}_i}{dt} + \frac{1}{k_B}\frac{\partial \Phi}{\partial \bar{\boldsymbol{q}}_i} = 0$$

- Equilibrium SM recovered when $\beta_i = \beta$, $\gamma_{ik} = \gamma_k$
- $\Phi \to \Phi_{\mathsf{MF}}$ meanfield approximation!

Non-equilibrium SM – Meanfield theory

- Space of trial *local Hamiltonians*: $\mathcal{H}_0$
- Free-entropy inequality: For all $\{h_0\} \in \mathcal{H}_0$,

  i) $\Phi \geq \Phi_0 - k_B\{\beta\}^T\{\langle h - h_0\rangle_0\} \equiv \mathcal{S}[\{h_0\}]$

  ii) $\Phi = \mathcal{S}[\{h_0\}] \Leftrightarrow \{h_0\} = \{h\}$

- Best approximation: $\Phi_{\mathsf{MF}} = \max_{\{h_0\}\in\mathcal{H}_0} \mathcal{S}[\{h_0\}]$
- Meanfield local equilibrium relations:

$$e_i = -\frac{1}{k_B}\frac{\partial \Phi_{\mathsf{MF}}}{\partial \beta_i}, \quad x_{ik} = \frac{1}{k_B}\frac{\partial \Phi_{\mathsf{MF}}}{\partial \gamma_{ik}}$$

- Meanfield mesoscopic dynamics:

$$\beta_i \frac{d\bar{\boldsymbol{q}}_i}{dt} = \frac{1}{k_B}\frac{\partial \Phi_{\mathsf{MF}}}{\partial \bar{\boldsymbol{p}}_i}, \quad \beta_i \frac{d\bar{\boldsymbol{p}}_i}{dt} = -\frac{1}{k_B}\frac{\partial \Phi_{\mathsf{MF}}}{\partial \bar{\boldsymbol{q}}_i}$$

Non-equilibrium SM – Meanfield theory

- Example: $\mathcal{H}_0 \equiv$ local harmonic oscillators,

$$h_{0i} = \frac{1}{2m(\boldsymbol{n}_i)}|\boldsymbol{p}_i - \bar{\boldsymbol{p}}_i|^2 + \frac{m(\boldsymbol{n}_i)\omega_i^2}{2}|\boldsymbol{q}_i - \bar{\boldsymbol{q}}_i|^2$$

- Entropy function (parameterized by $\{\omega\}$):

$$\Phi_{\mathsf{MF}} = \sum_{i=1}^{N} k_B \left(\frac{\beta_i}{2m_i}|\bar{\boldsymbol{p}}_i|^2 + \beta_i \langle V_i \rangle_0 + 3\log(\hbar\beta_i\omega_i) - 3 \right)$$

Gaussian integrals!
Hermite quadrature!

- Meanfield mesoscopic dynamics:

$$\dot{\bar{\boldsymbol{q}}}_i = \frac{\bar{\boldsymbol{p}}_i}{m_i}, \quad \dot{\bar{\boldsymbol{p}}}_i = -\frac{\partial}{\partial \bar{\boldsymbol{q}}_i} \sum_{j=1}^{N} \langle V_j \rangle_0,$$

- Meanfield optimality: $\dfrac{\partial}{\partial \omega_i} \displaystyle\sum_{j=1}^{N} \beta_j \langle V_j \rangle_0 + \frac{3}{\omega_i} = 0$

Non-equilibrium SM – Kinetics

- Need equations of evolution for $\{\beta\}$ and $\{\gamma\}$
- Local conservation equations:

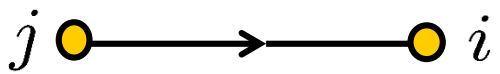

$$\underbrace{\dot{e}_i = \dot{w}_i + \boldsymbol{\mu}_i^T \dot{\boldsymbol{x}}_i + \sum_{j \neq i} R_{ij},}_{\text{energy}} \qquad \underbrace{\dot{\boldsymbol{x}}_i = \sum_{j \neq i} \boldsymbol{J}_{ij}}_{\text{mass}}$$

- Local dissipation inequality:

$$\Sigma_{ij} = k_B(\beta_i - \beta_j)R_{ij} + k_B(\boldsymbol{\gamma}_i - \boldsymbol{\gamma}_j) \cdot \boldsymbol{J}_{ij} \geq 0$$

- General kinetic relations: calibrate from exp. data!

$$\underbrace{R_{ij} = f(\beta_i - \beta_j),}_{\text{Discrete Fourier law}} \qquad \underbrace{\boldsymbol{J}_{ij} = g(\boldsymbol{\gamma}_i - \boldsymbol{\gamma}_j)}_{\text{Discrete Fick's law}}$$

Non-equilibrium SM – Sample potentials

- Structure of typical multispecies EAM potential:

$$V = \sum_{i=1}^{N} \left[n_i F_i(\rho_i) + \frac{1}{2} \sum_{j \neq i} n_i n_j S_{ij}(n_i, n_j) \phi_{ij}(r_{ij}) \right]$$

- Meanfield equilibrium: $\mu_i = \frac{k_B T}{2} \log \frac{x_i}{1 - x_i}$

- Master equation: $\frac{\partial x_i}{\partial t} = \sum_{\langle i,j \rangle} (\psi_{j \to i} - \psi_{i \to j})$

- Transition probabilities:

$$\psi_{i \to j} = \nu_i \, x_j (1 - x_i) \, e^{-\beta \left(E_{i \to j} + (\mu_i - \mu_j)/2 \right)}$$

attempt frequency

energy barrier

MD *vs*. DMD in pictures

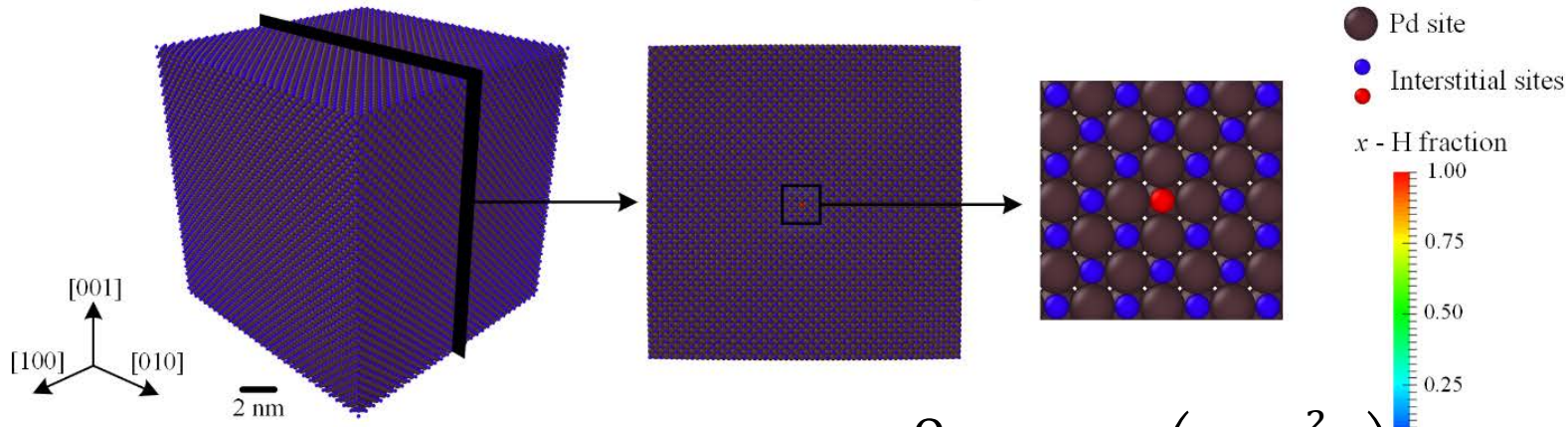

Random walk model: $x(r,t) = \dfrac{\Omega}{(4\pi D_{\mathrm{H}} t)^{3/2}} \exp\left(-\dfrac{r^2}{4\pi D_{\mathrm{H}}}\right)$

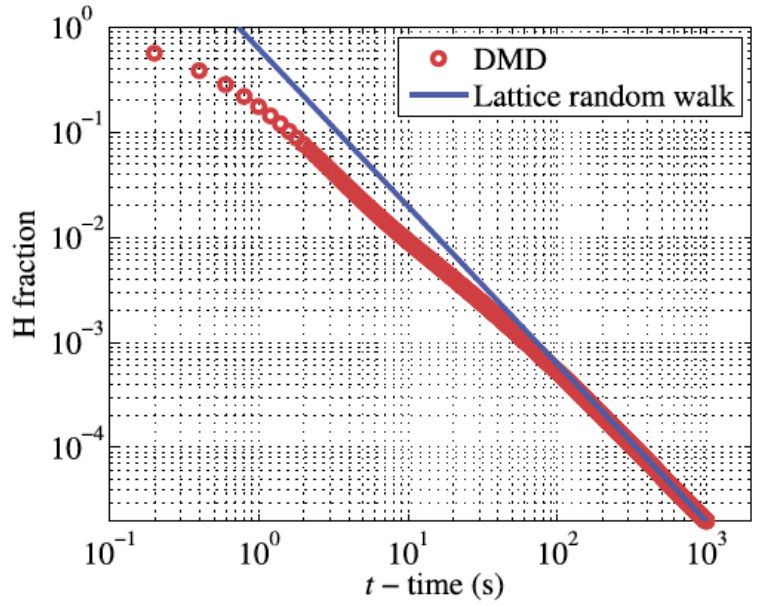

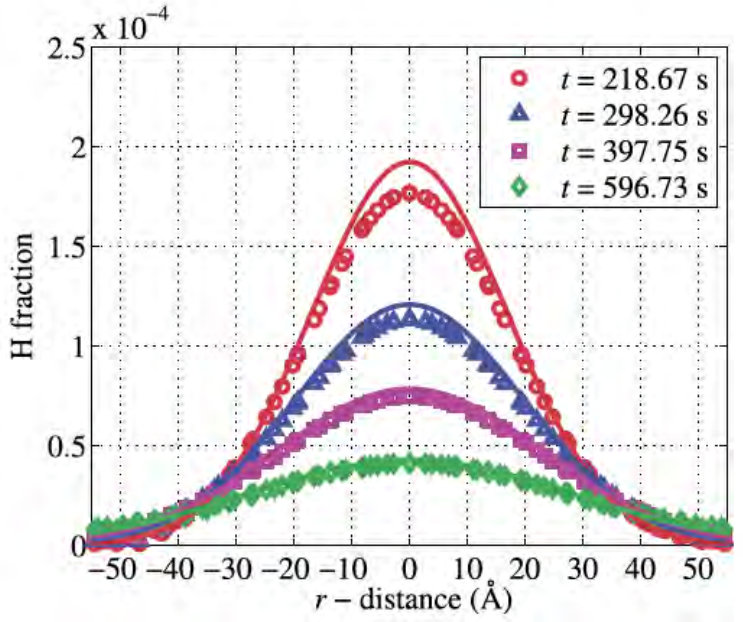

X. Sun, M. P. Ariza, M. Ortiz, K. G. Wang, J Comput Phys, **350**:470-492, 2017.

Application: Lithium-ion batteries

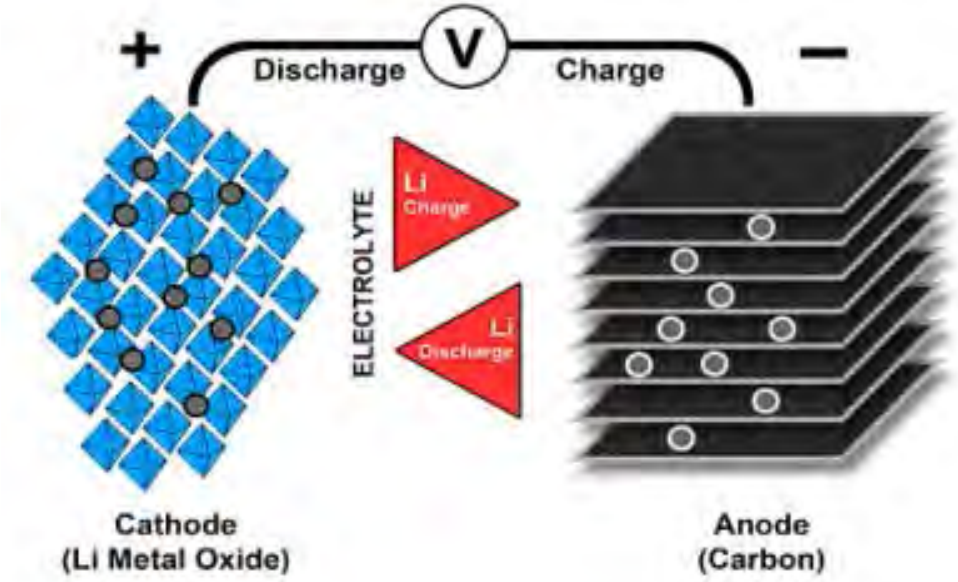

http://batteryuniversity.com/learn/article/lithium_based_batteries

Nano-Micro Lett. (2014) 6(4):347–358

Element	Gravimetric capacity (mAh g^{-1})	Volumetric capacity (mAh cm^{-3})	Cost	Toxicity	Safety
Si	4,200	2,400	Low	No	High
C	372	890	Low	No	Low
Ge	1,568	2,300	High	High	High
Sn	990	2,020	Low	No	High
P	2,600	2,250	Low	High	Low
Sb	660	1,890	Low	High	Low
Pb	549	1,790	Low	High	Low

- Si-based anodes offer the highest specific capacity (ten time the specific capacity of graphite)
- But: 300% expansion during charging (lithiation)
- Si undergoes amorphization upon lithiation
- Mechanical failure (pulverization) after a few cycles…

Nano-engineered Si anodes

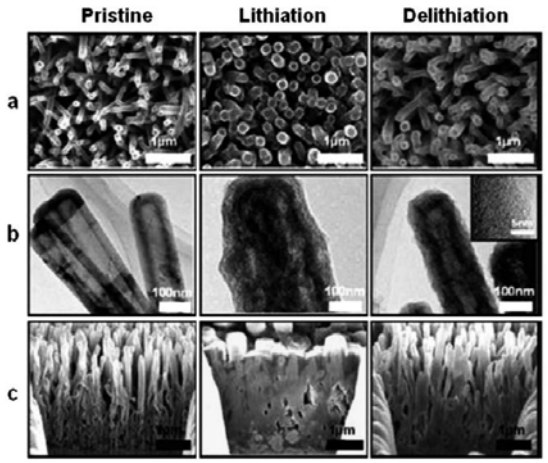

Si-nanowire anodes, lithiation-delithiation[1]

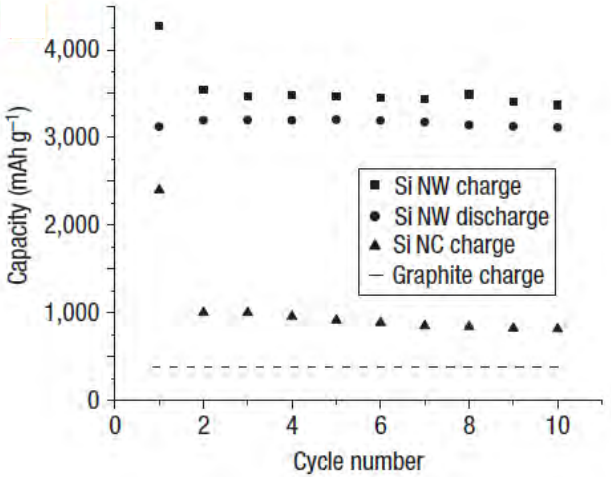

Si-nanowire anodes, capacity *vs*. #cycles[2]

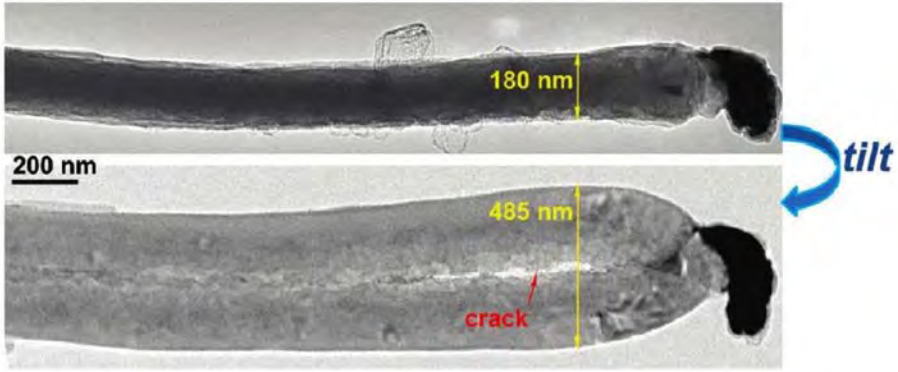

Lithiation of Si nanowire[3]

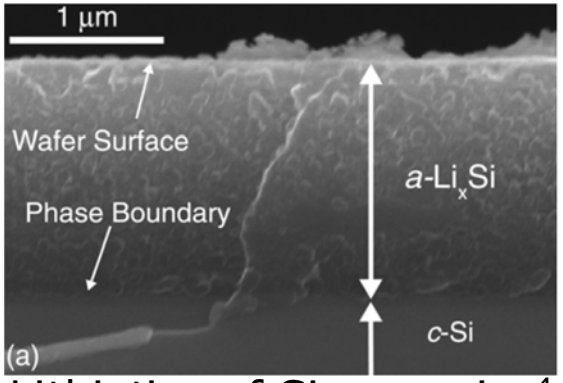

Lithiation of Si nanowire[4]

[1]T. Song *et. al.*, *Nano Lett*ers, **10**(5) (2010) 1710–1716.
[2]C.K. Chan *et al.*, *Nature Nanotech.*, **3** (2008) 31-35.
[3]X.H. Liu and H. Zheng, *Nano Letters*, **11**(8) (2011) 3312-3318.
[4]M.J. Chon *et al.*, *Phys. Rev. Lett.*, **107**(4) (2011) 045503.

Michael Ortiz
MPIE 2018

Si lithiation model

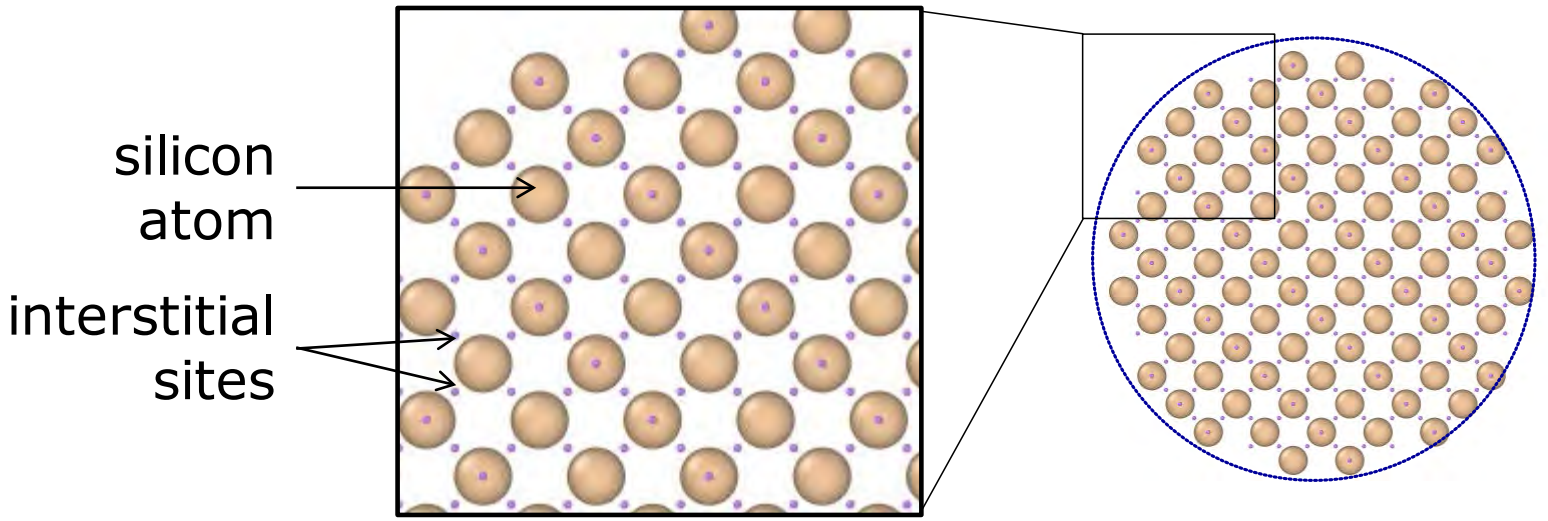

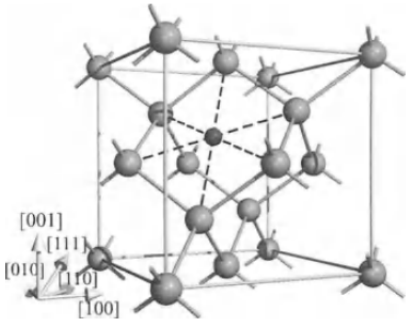

Hexagonal interstitial:
2 interst./Si atom

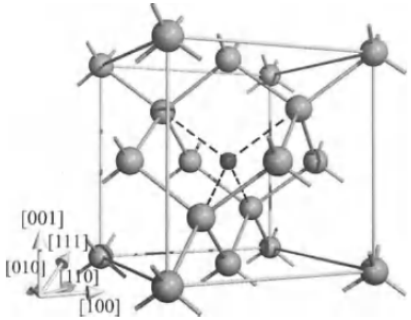

Tetrahedral interstitial:
1 interst./Si atom

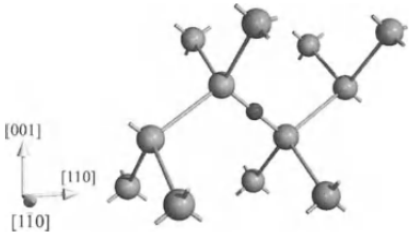

Bond-centered interstitial:
2 interst./Si atom

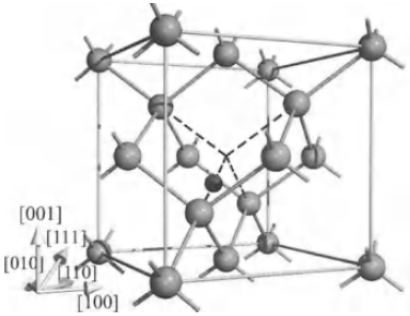

Anti-bond interstitial:
4 interst./Si atom

Interstitial sites of diamond Si

P. Pitchler, Intrinsic Point Defecs, Interstitials and their Diffusion in Si, Springer-Verlag Wien, 2004.

Michael Ortiz
MPIE 2018

Si nanowire lithiation simulations

- Si nanowire @ Li saturation on outer boundary
  - *2NN MEAM for Si-Li*[1]
  - *T = 300K*
  - *Master transport equation*[2]
  - *Diffusion parameters:*
    - *v = 1013 1/s*
    - *ΔE = 0.55 eV*
  - *5 interstitials/atom*

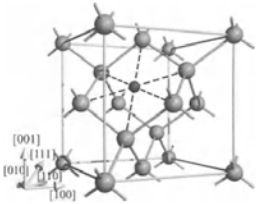

Hexagonal interstitial:
2 interst./Si atom

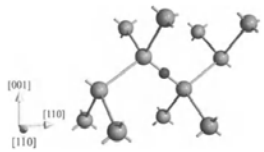

Bond-centered interstitial:
2 interst./Si atom

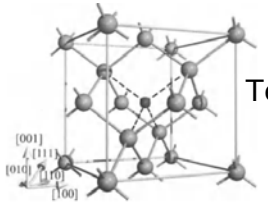

Tetrahedral interstitial:
1 interst./Si atom

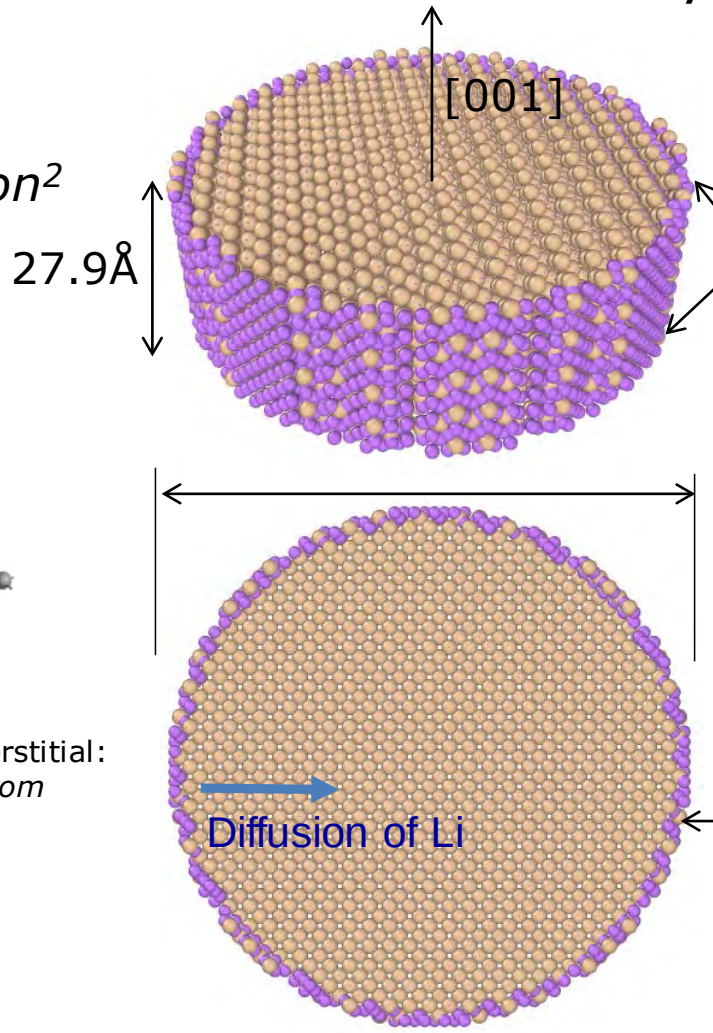

10,126 Si atoms,
50,565 interstitials

[1]Z. Cui et al., *J. Power Sources*, **207** (2012) 150–159.
[2]F. Zhang and W. A. Curtin, MSMSE 16, 055006 (2008).

Si lithiation model - Validation

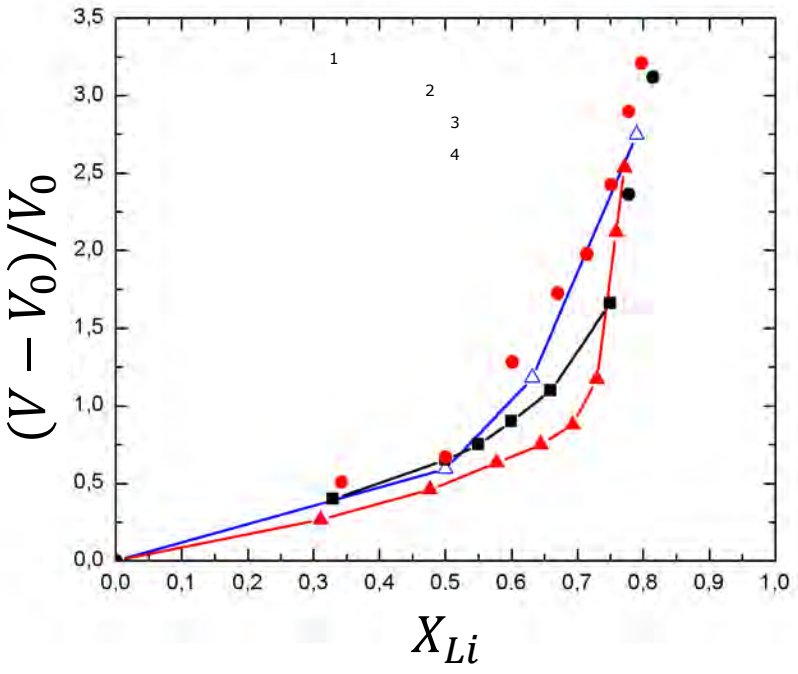

Volume expansion
vs. Li molar fraction

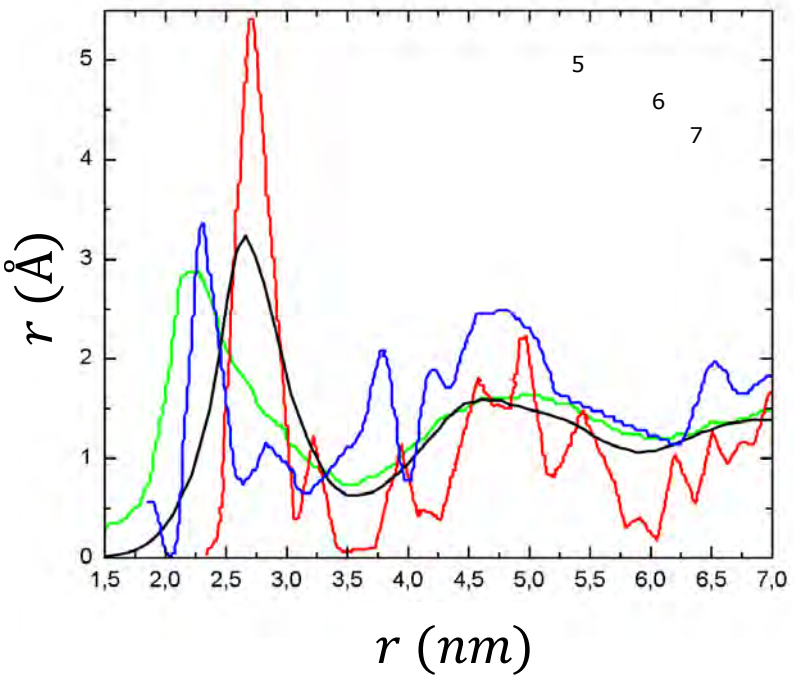

Radial distribution function
at full lithiation

[1]P. Johari *et al*., *Nano Lett.*, **11**(12) (2011) 5494–5500.
[2]H.S. Lee and B.J. Lee, *Met. Mater. Int*., **20**(6) (2014), 1003-1009.
[3]L.Y. Beaulieu *et al*., *Electrochem. Solid-State Lett.*, **4**(9) (2001) A137-A140.
[4]L.Y. Beaulieu *et al*., *J. Electrochem. Soc*., **150**(11) (2003) A1457-64.
F. Fan *et al*., *Modelling Simul. Mater. Sci. Eng.*, **21** (2013) 074002.
V.L. Chevrier and J.R. Dahn, *J. Electrochem. Soc.*, **156**(6) (2009) A454-A458.
B. Key *et al*., *J. Am. Chem. Soc*., **133** (2010) 503-512.

Si nanopillar lithiation – Atomic fractions

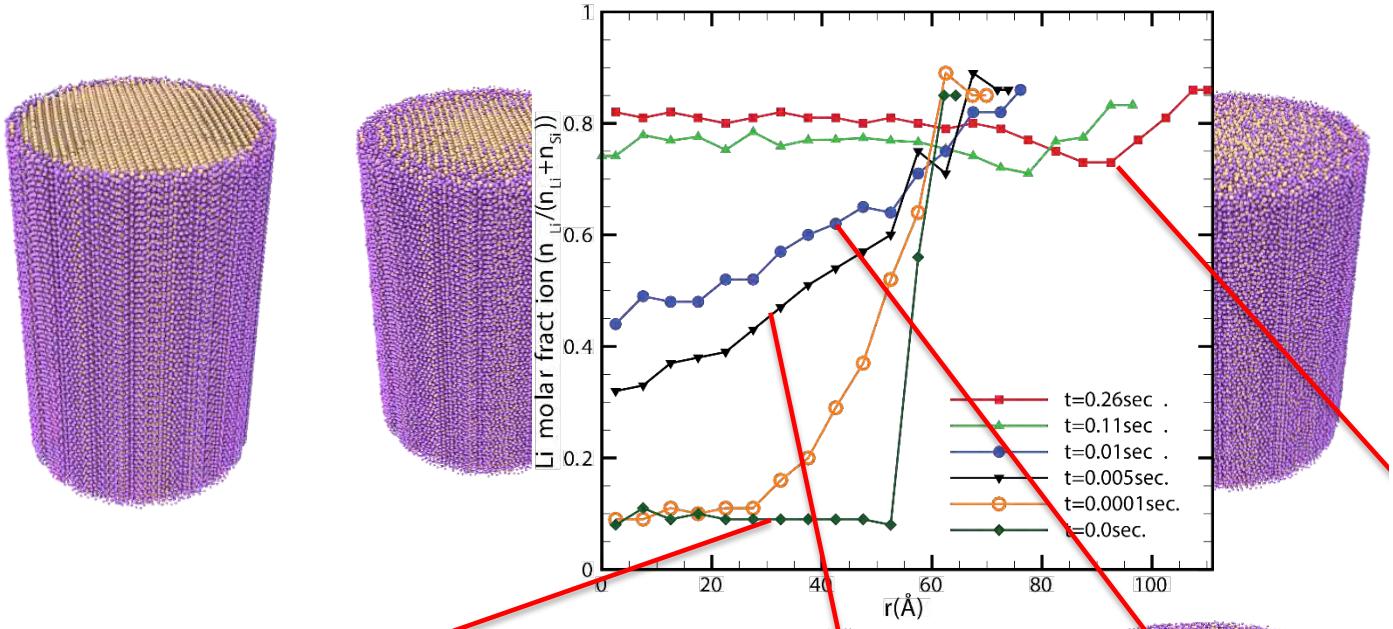

Fully lithiated

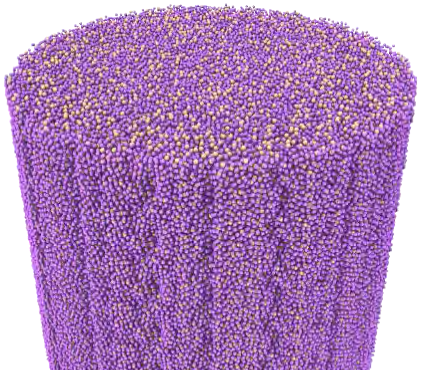

Average Li atomic molar fraction ~ 0.79

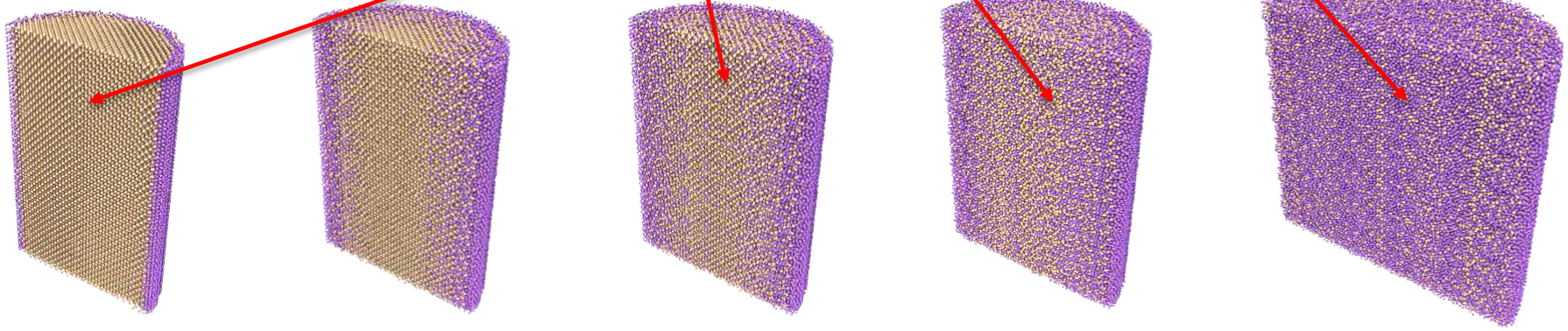

0.0 ms | 0.8 ms | 5 ms | 10 ms | 260 ms

Si atoms

Li atoms

J.P. Mendez, M. Ponga, M. Ortiz, *JMPS*, **115** (2018) 123-141.

Michael Ortiz
MPIE 2018

Si nanopillar lithiation – Volume

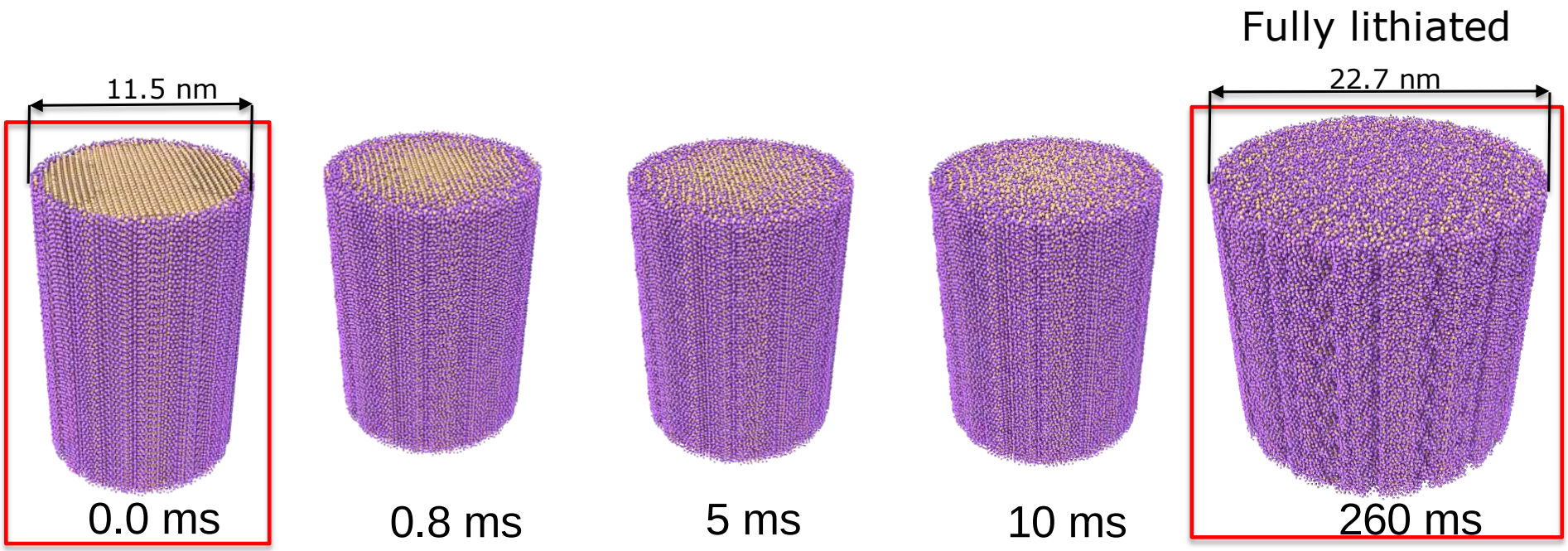

Si atoms

Li atoms

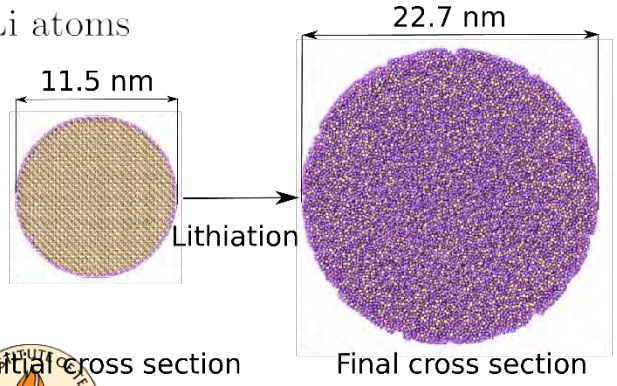

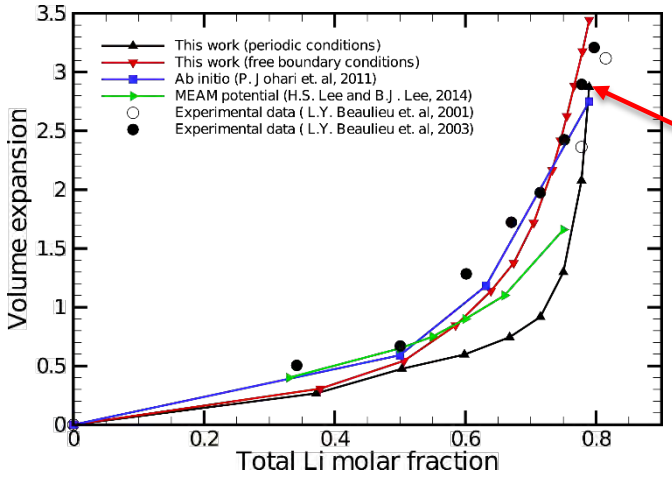

Volume expansion of 287%

J.P. Mendez, M. Ponga, M. Ortiz, *JMPS*, **115** (2018) 123-141.

Michael Ortiz
MPIE 2018

Si nanopillar lithiation – Interface

Fully lithiated

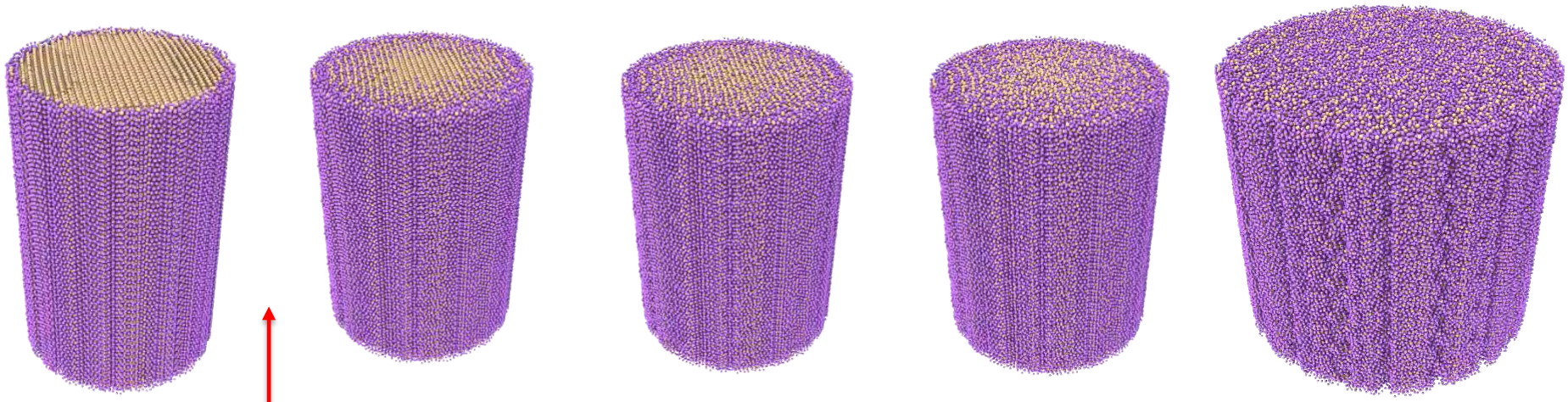

0.0 ms | 0.8 ms | 5 ms | 10 ms | 260 ms

Si atoms

Li atoms

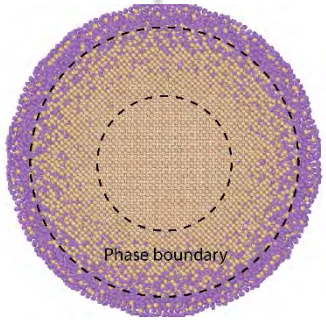

0.1 ms

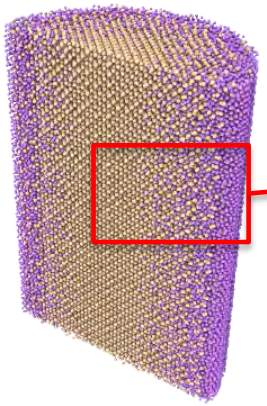

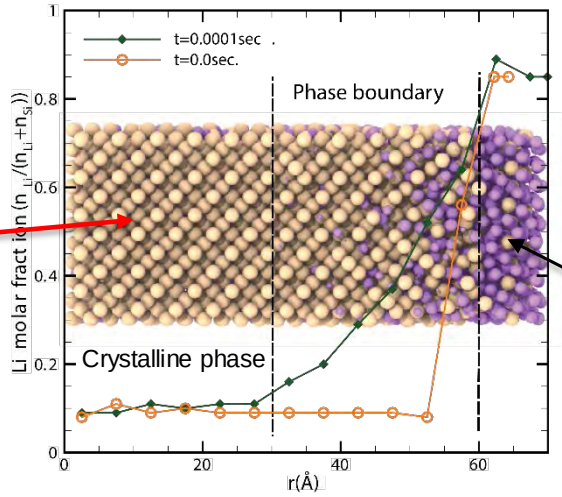

Phase boundary ~ 20Å

Amorphous phase

J.P. Mendez, M. Ponga, M. Ortiz, *JMPS*, **115** (2018) 123-141.

Michael Ortiz
MPIE 2018

Si nanopillar lithiation – Amorphization

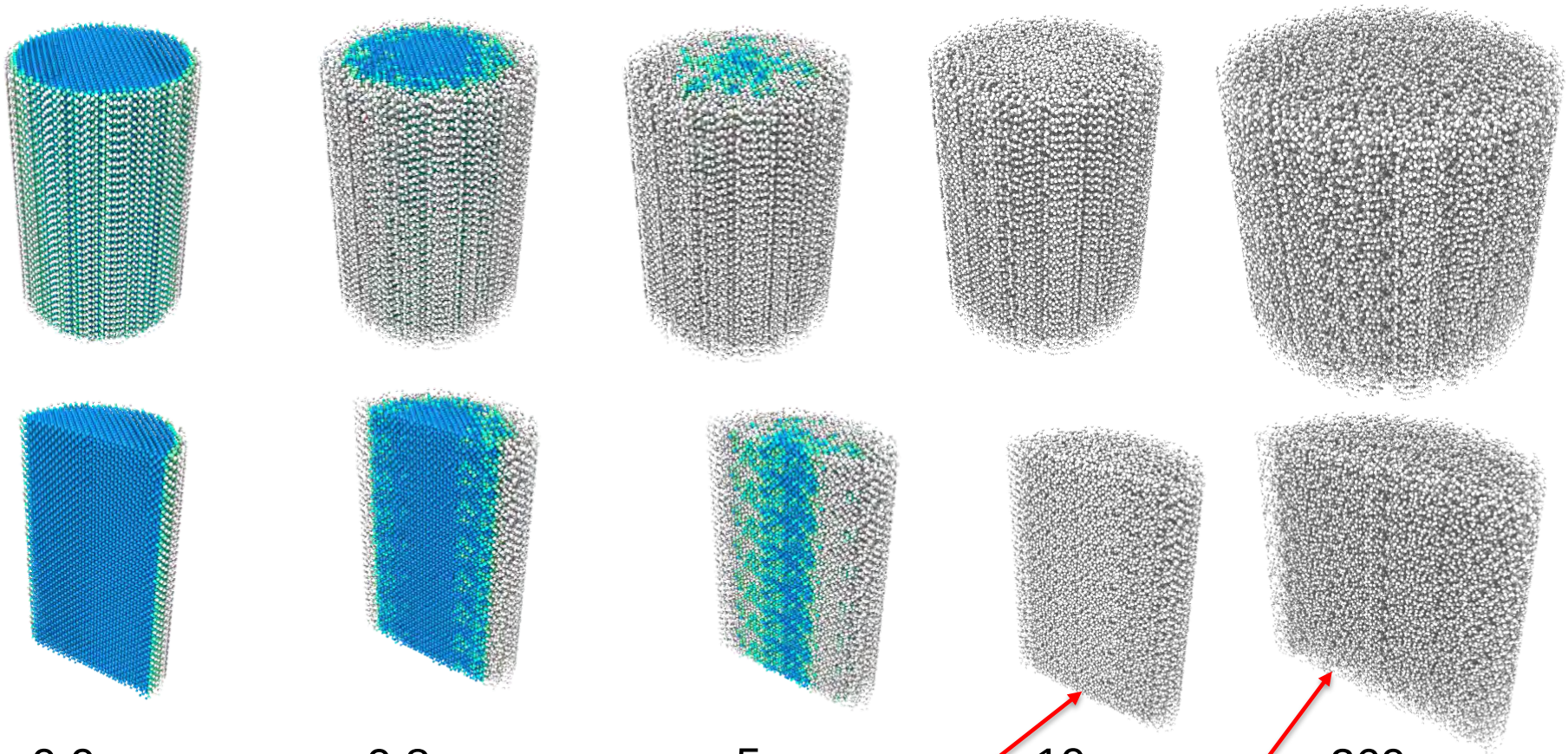

J.P. Mendez, M. Ponga, M. Ortiz,
JMPS, **115** (2018) 123-141.

Michael Ortiz
MPIE 2018

Si nanopillar lithiation – Amorphization

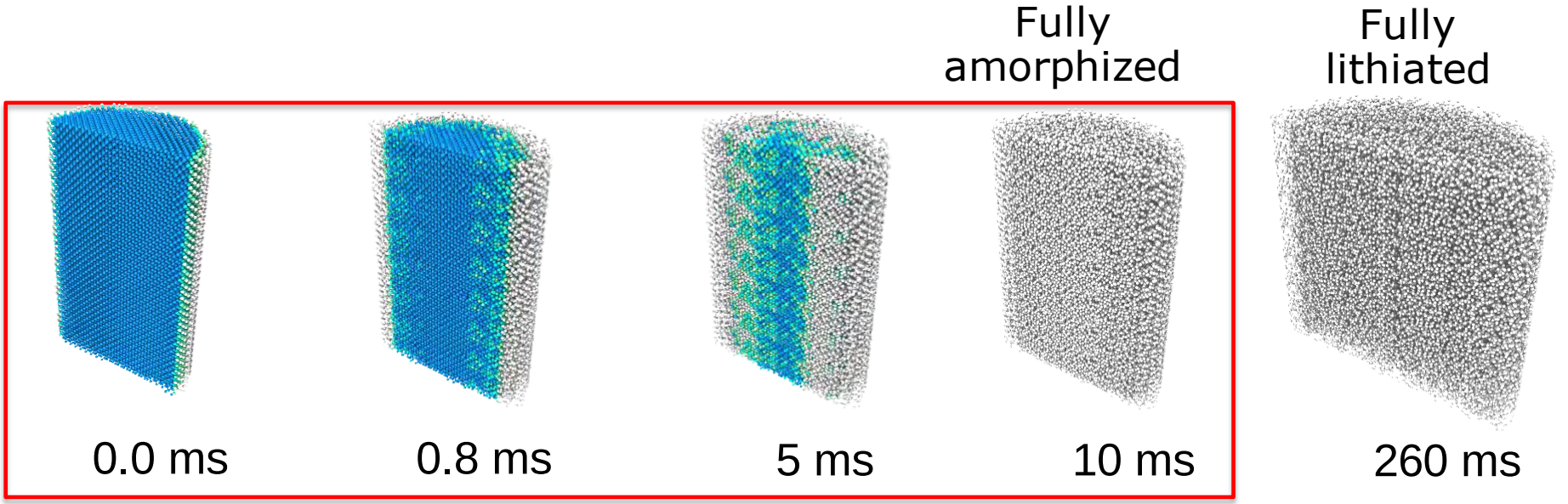

Amorphous
Cubic diamond
Cubic diamond (1st neighbor)
Cubic diamond (2st neighbor)

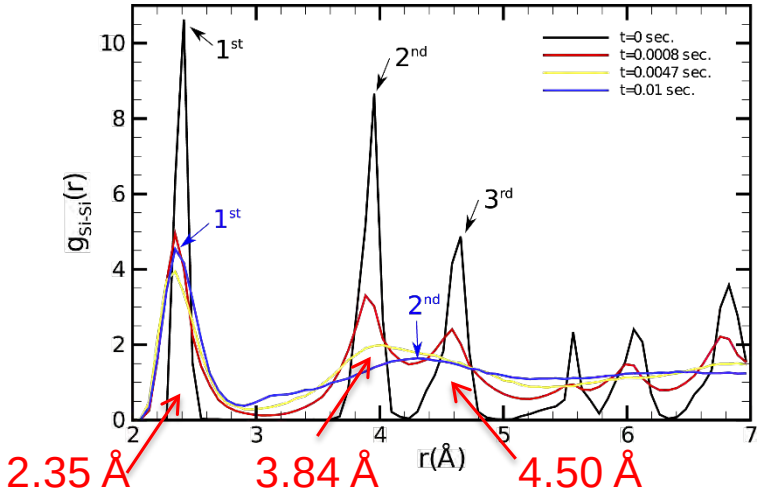

radial distribution function

J.P. Mendez, M. Ponga, M. Ortiz, *JMPS*, **115** (2018) 123-141.

Michael Ortiz
MPIE 2018

Si nanopillar lithiation – Amorphization

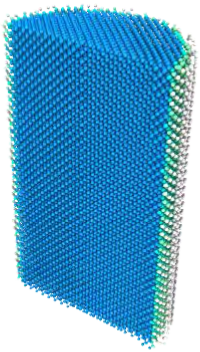

0.0 ms

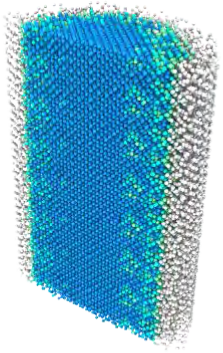

0.8 ms

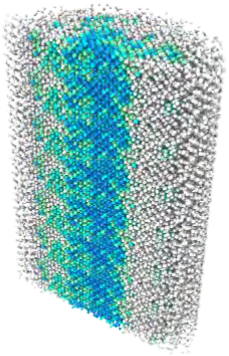

5 ms

Fully amorphized

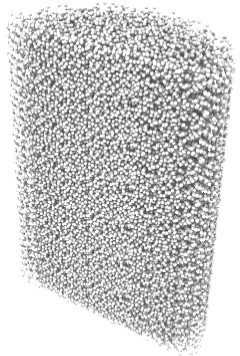

10 ms

Fully lithiated

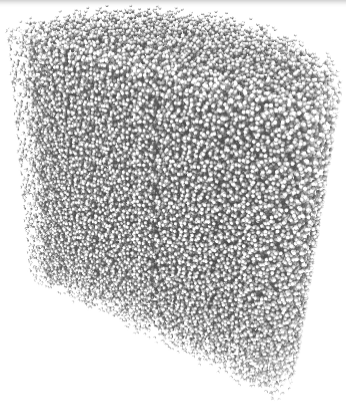

260 ms

Amorphous

Cubic diamond

Cubic diamond (1st neighbor)

Cubic diamond (2st neighbor)

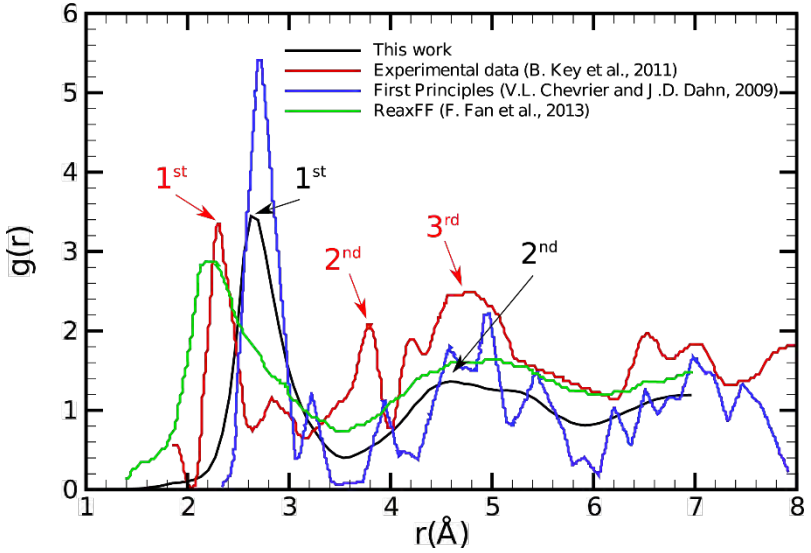

Michael Ortiz
MPIE 2018

J.P. Mendez, M. Ponga, M. Ortiz, *JMPS*, **115** (2018) 123-141.

Si nanopillar lithiation – Porosity

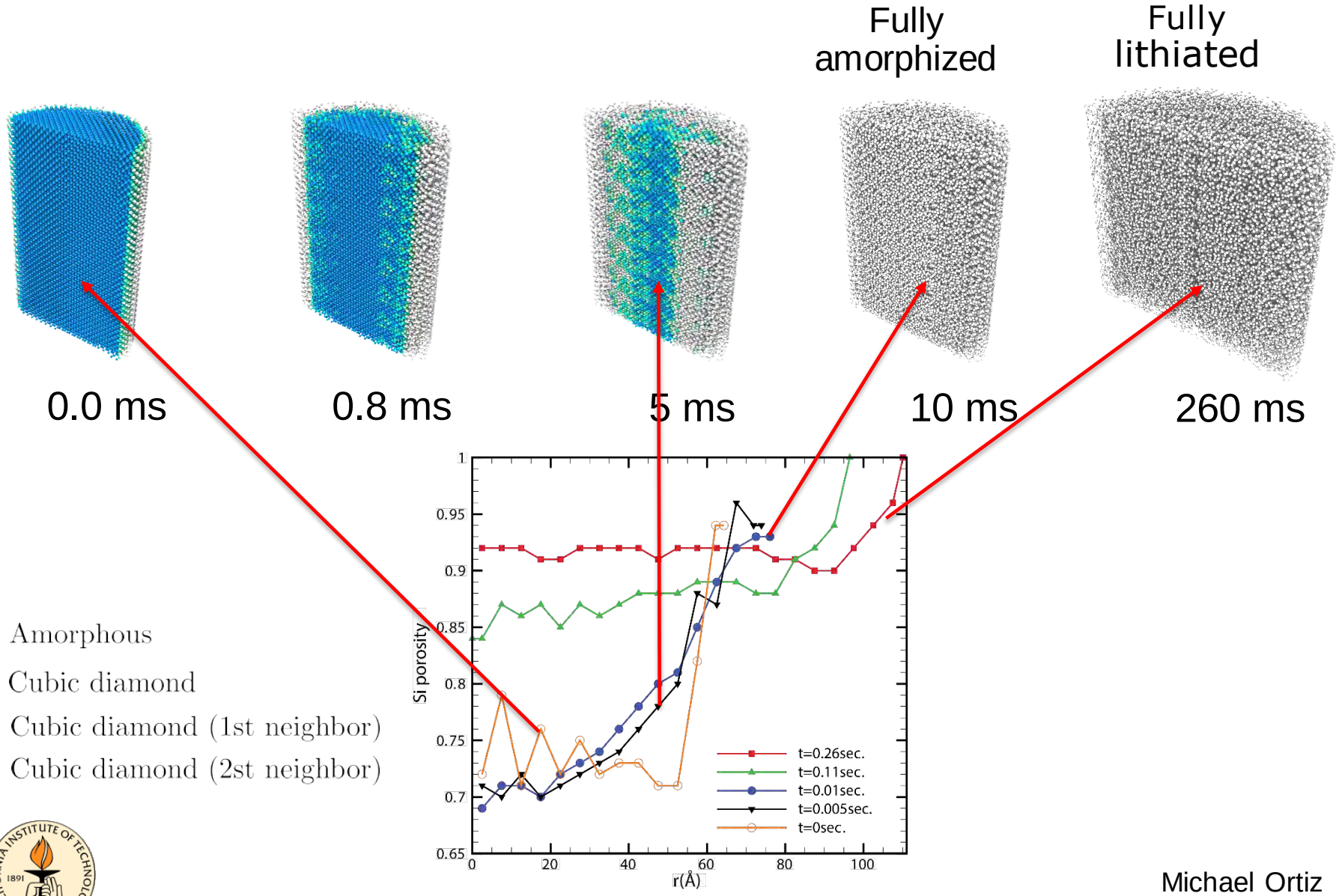

Michael Ortiz
MPIE 2018

J.P. Mendez, M. Ponga, M. Ortiz, *JMPS*, **115** (2018) 123-141.

Application: Hydrogen storage in Pd

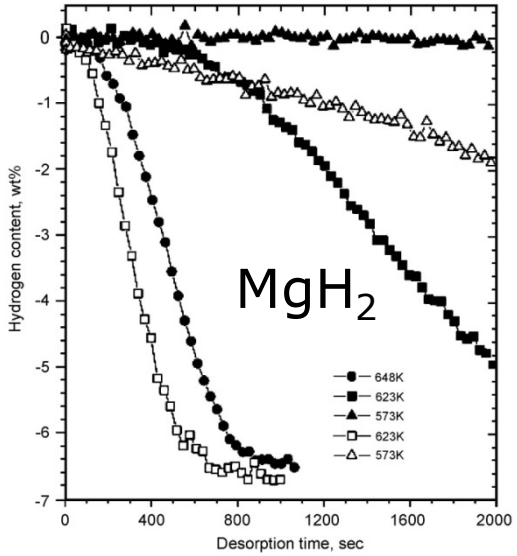

- Hydrogen storage is a key element of the hydrogen economy…
- Typical absorption/desorption times are temperature/pressure dependent and in hour range[1]
- Outlook: Store hydrogen in nanostructured metals (particles, nanowires)

- But: Structural effects,
  - *Volume expansion*
  - *Pulverization*
- Mg disintegrates after 10 hydration cycles[2]
- Predictive capability:
  - *Atomistic realism*
  - *Long-time behavior…*

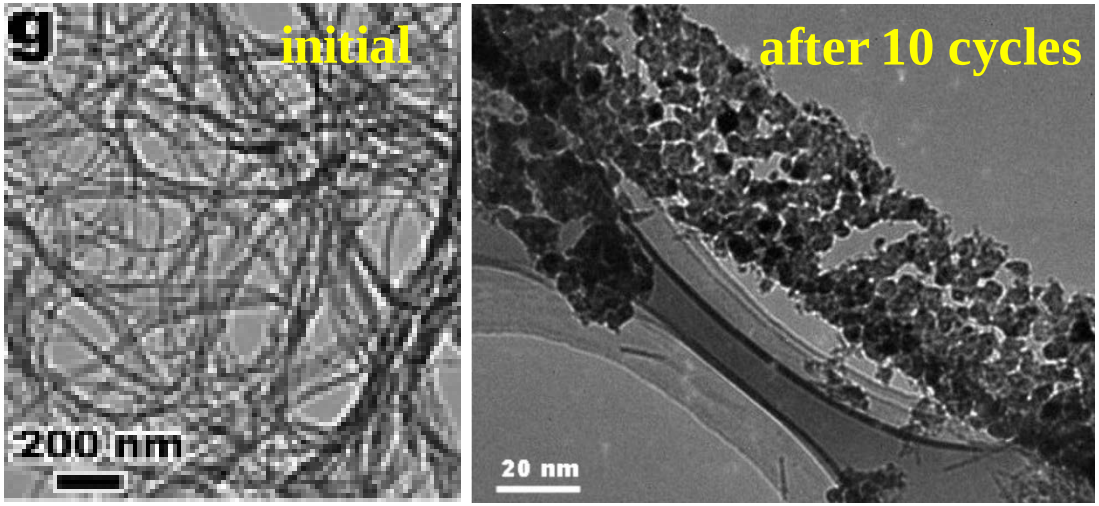

[1]B. Sakintuna, F. Darkrim and M. Hirscher, *Int.J. Hydrogen Energy*, **32** (2007) 1121– 1140.
[2]W. Li, C. Li et al., J. Am. Chem. Soc., 2007

H storage in Pd NW – α–β interface

- PdH_x exists in two phases at room temperature:
  - α phase: $0 < x \leq 0.03$
  - β phase: $0.608 \leq x \leq 1$
- In both phases: H occupies octahedral sites of FCC Pd lattice
- Phase transition ($\alpha \rightarrow \beta$): 10.4% volume expansion
- Computational setup: EAM potential[1], NN transport kinetics

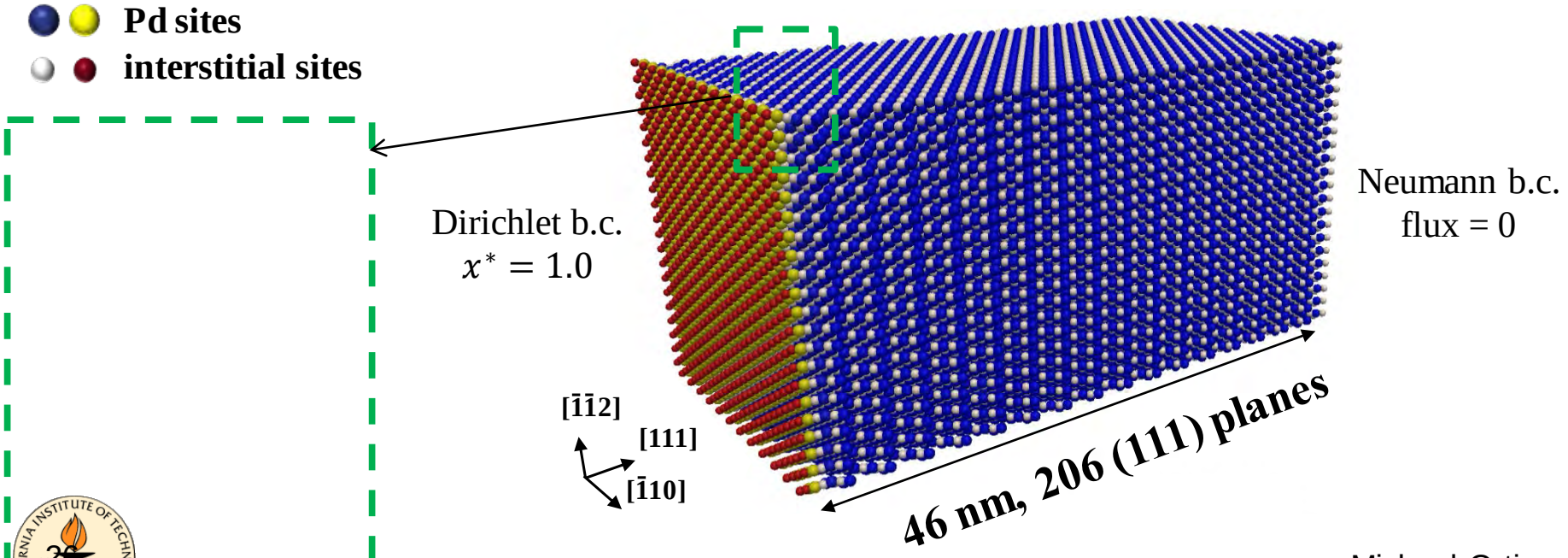

[1]X. Zhou, J. Zimmerman *et al.*, *J. Mater. Res.*, 2008

H storage in Pd NW – α–β interface

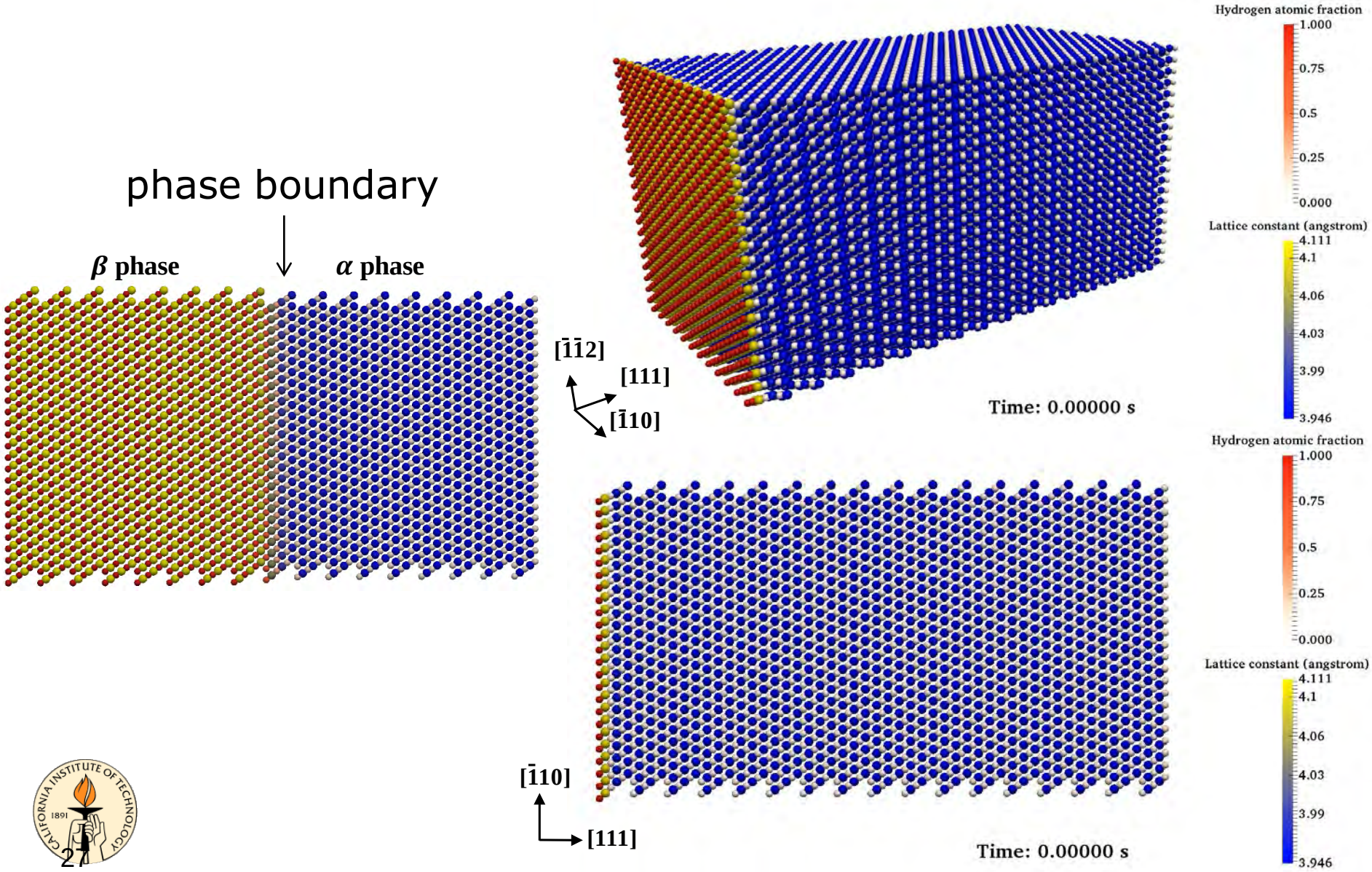

H storage in Pd NW – α–β interface

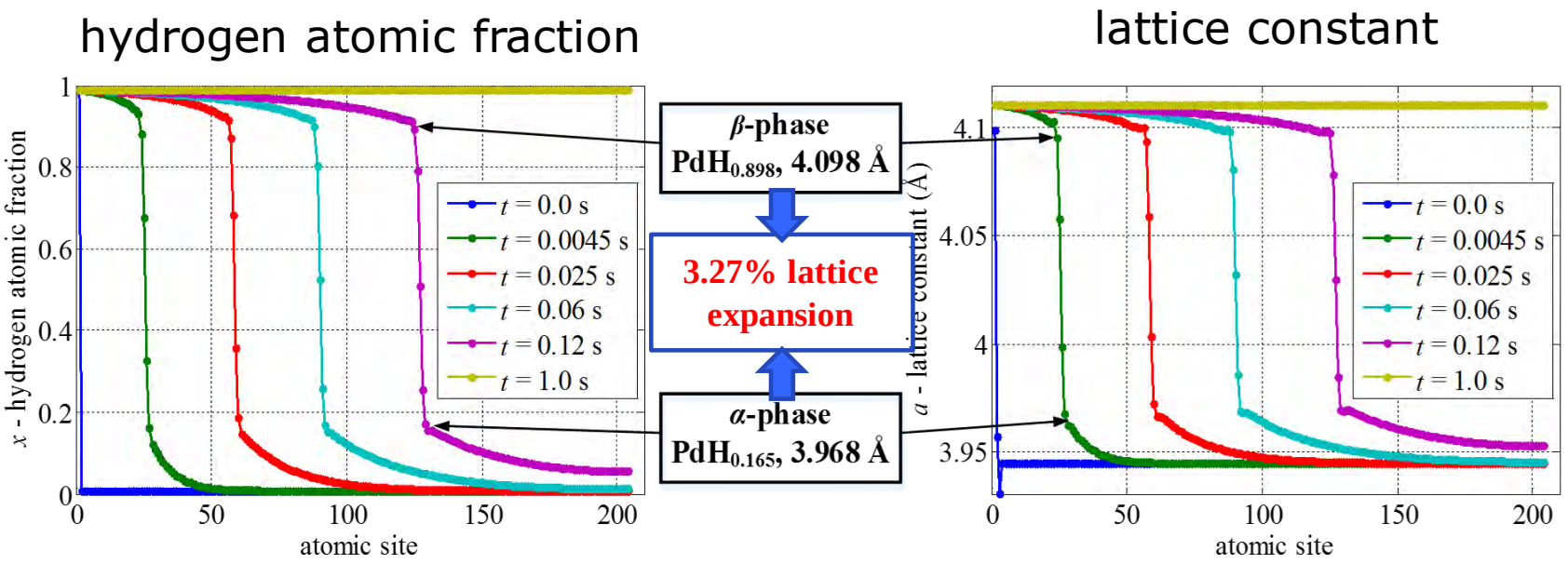

- Phase transition predicted (3.27% *vs.* 3.35%)
- Phase boundary motion, velocity, predicted (~100 nm/s)
- In progress: MgH_2 (hcp α-phase, rutile β-phase)

Sun, X., Ariza, M.P., Ortiz, M. and Wang, K., *Int J Hydrogen Energy*, 2018;**43**(11):5657-67.

Application: H storage in Pd nanoparticles

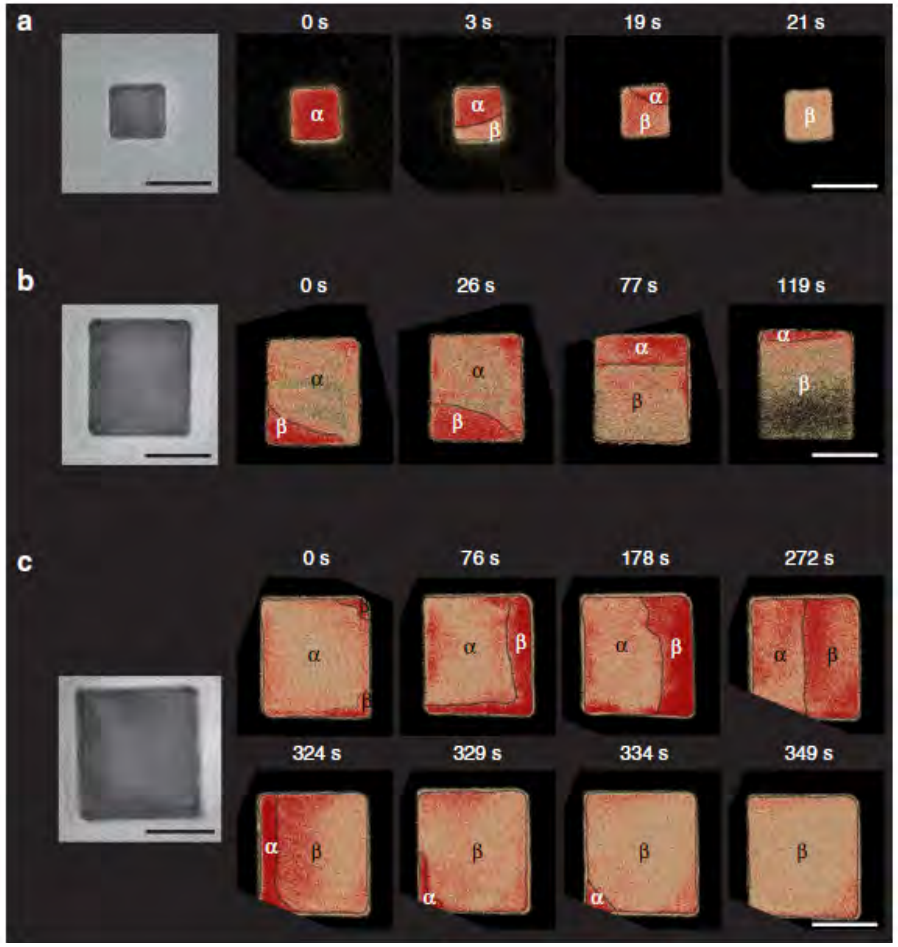

20 nm

36 nm

43 nm

STEM frames showing α to β phase evolution

Narayan *et al.*, *Nature Comm.* (2017)| DOI: 10.1038/ncomms14020)

H storage in Pd NP – Problem setup

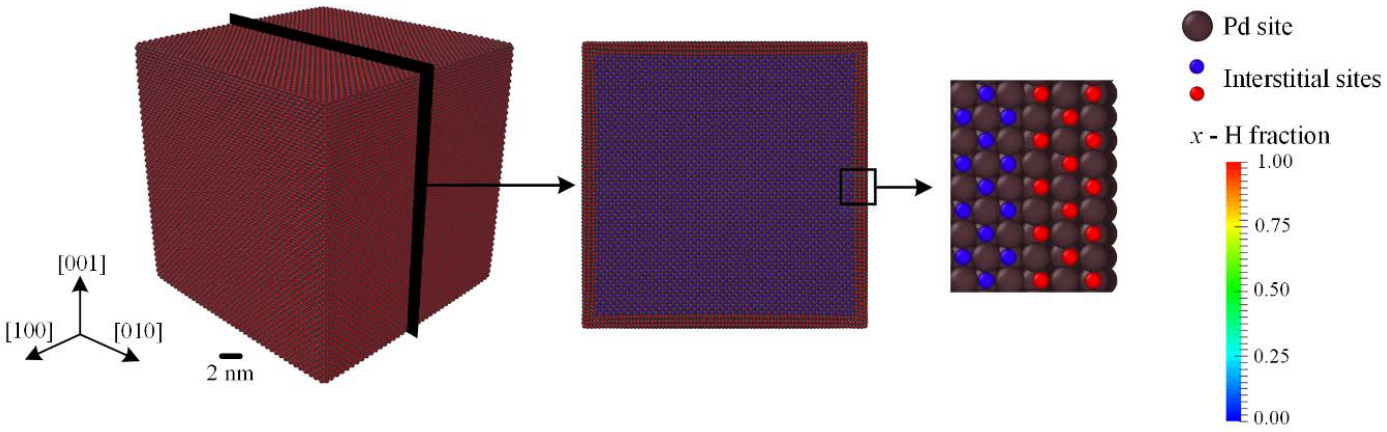

Nanocube (edge length: 16 nm), with faces on {100} planes.

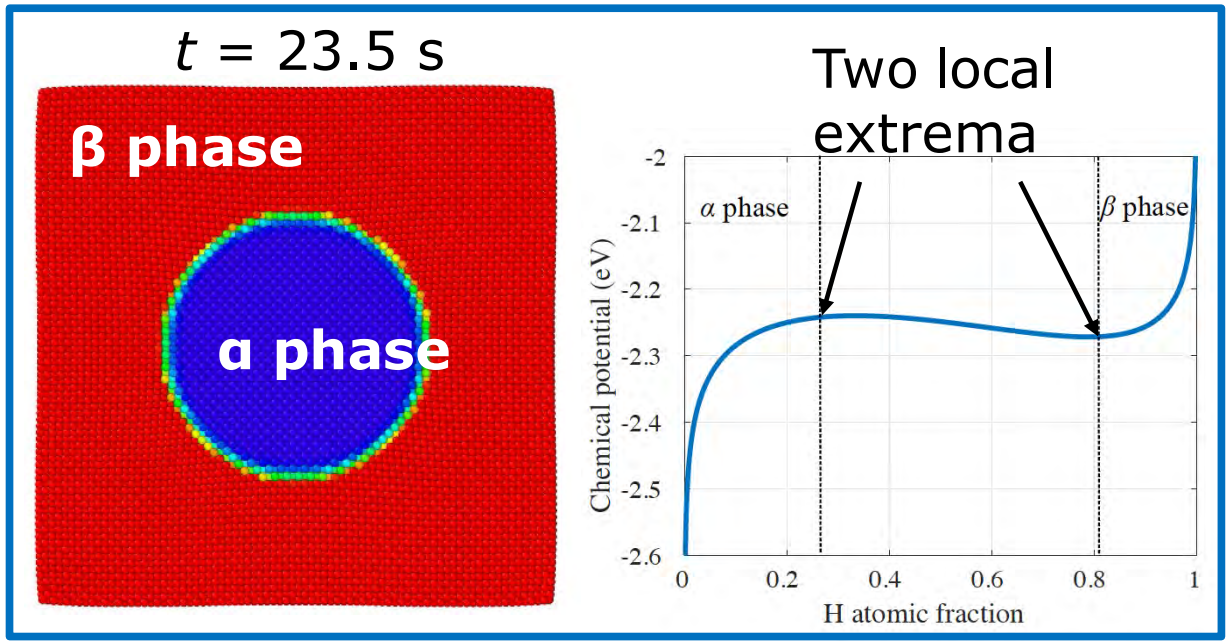

X. Sun, M. P. Ariza, M. Ortiz, K. G. Wang, *JMPS* (submitted).

H storage in Pd NP – Interfacial strain

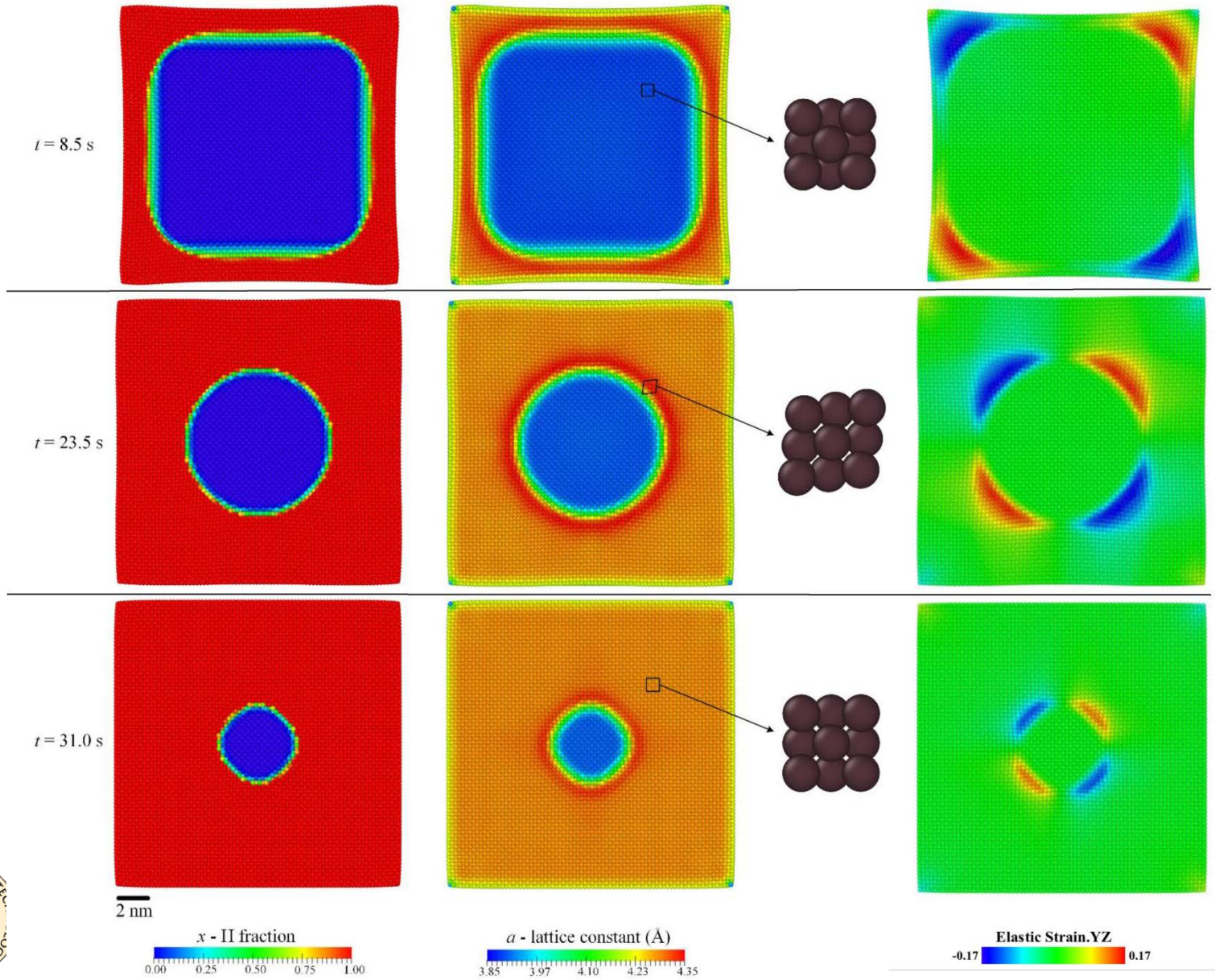

el Ortiz
: 2018

Interfacial dislocations

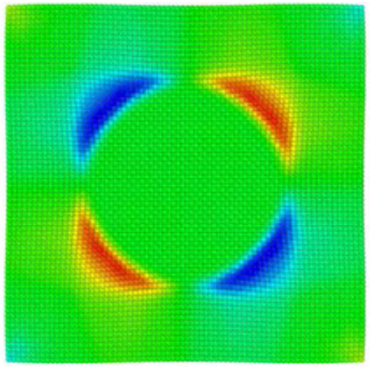

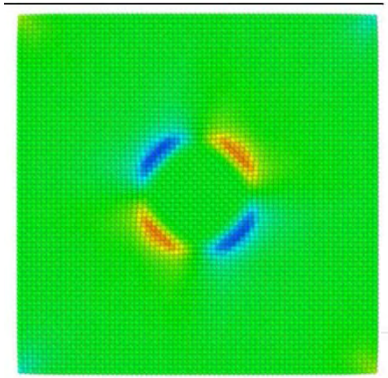

misfit strain evolution

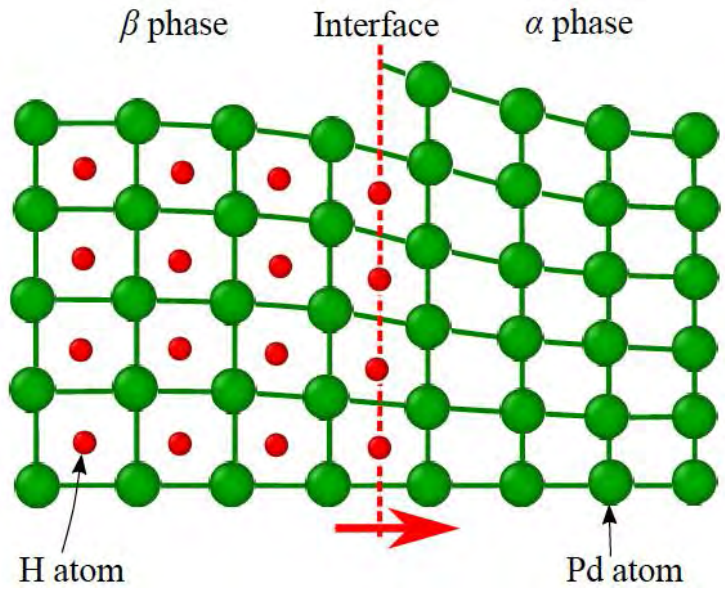

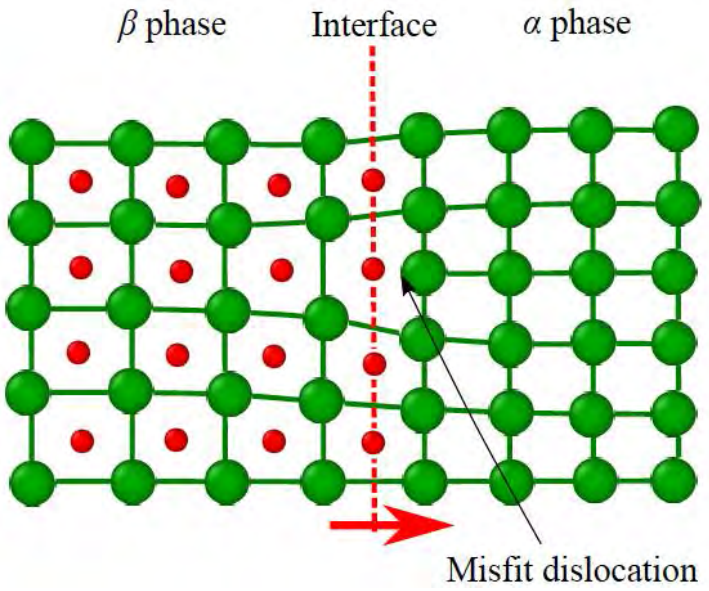

Misfit strain is relieved by misfit dislocations

X. Sun, M. P. Ariza, M. Ortiz, K. G. Wang, *JMPS* (submitted).

PdH: Interfacial misfit dislocations

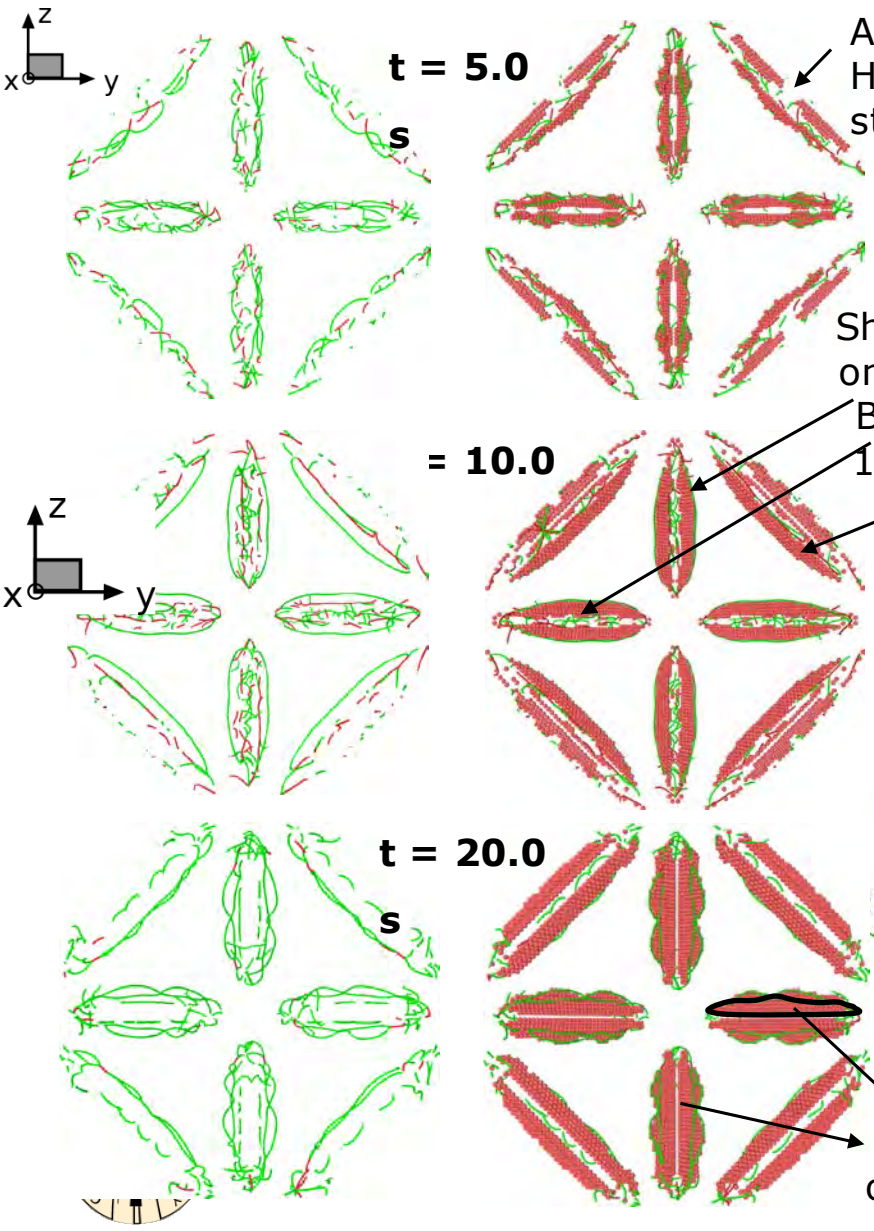

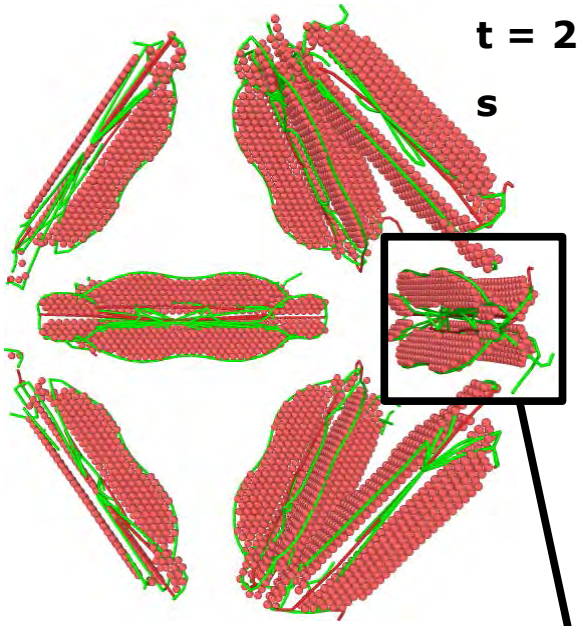

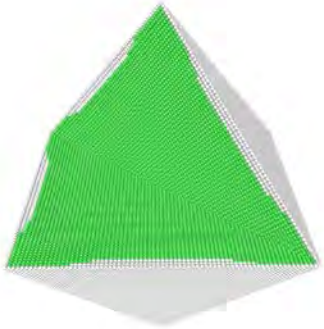

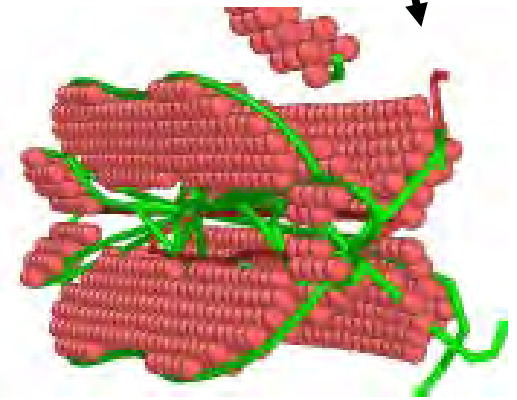

Michael Ortiz
MPIE 2018

PdH: Interfacial misfit dislocations

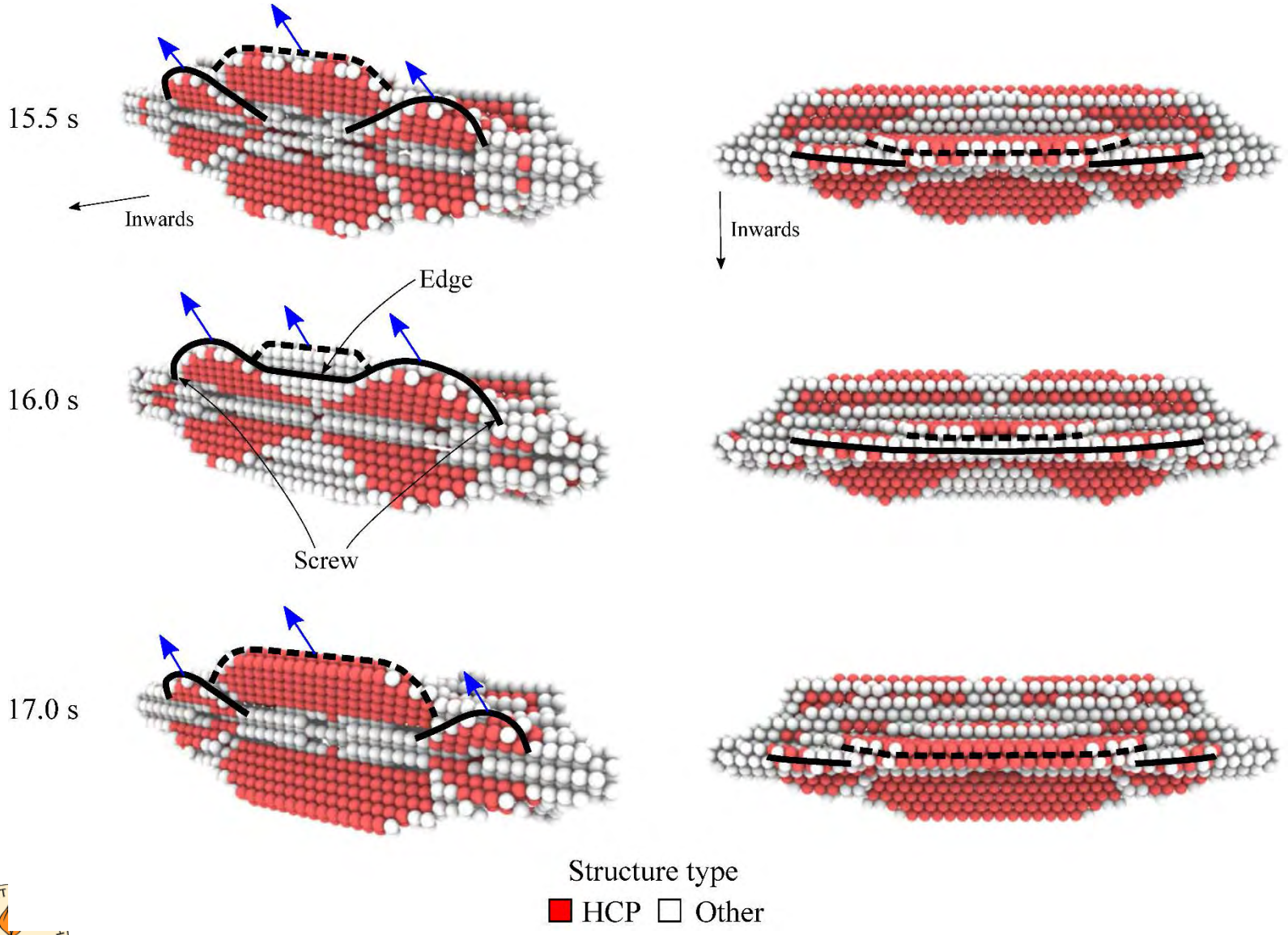

X. Sun, M. P. Ariza, M. Ortiz, K. G. Wang, *JMPS* (submitted).

PdH: Interfacial misfit dislocations

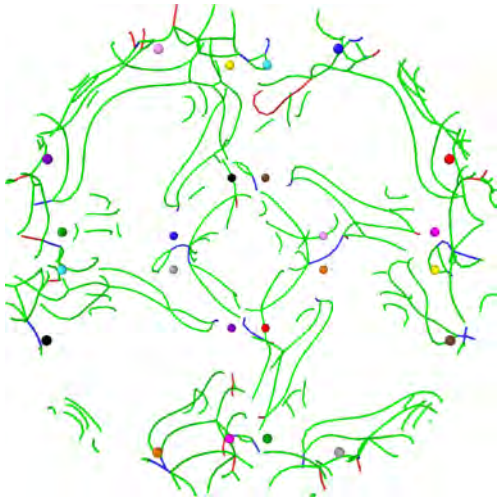

(100) plane

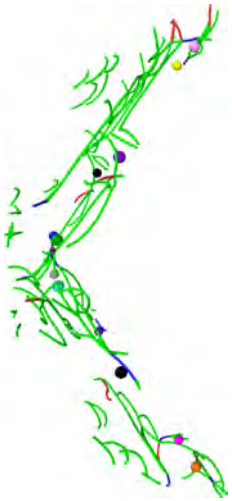

(111) direction

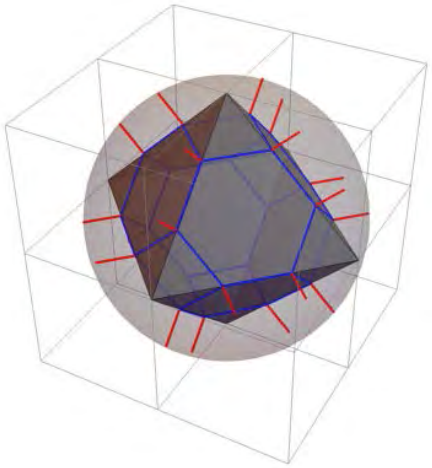

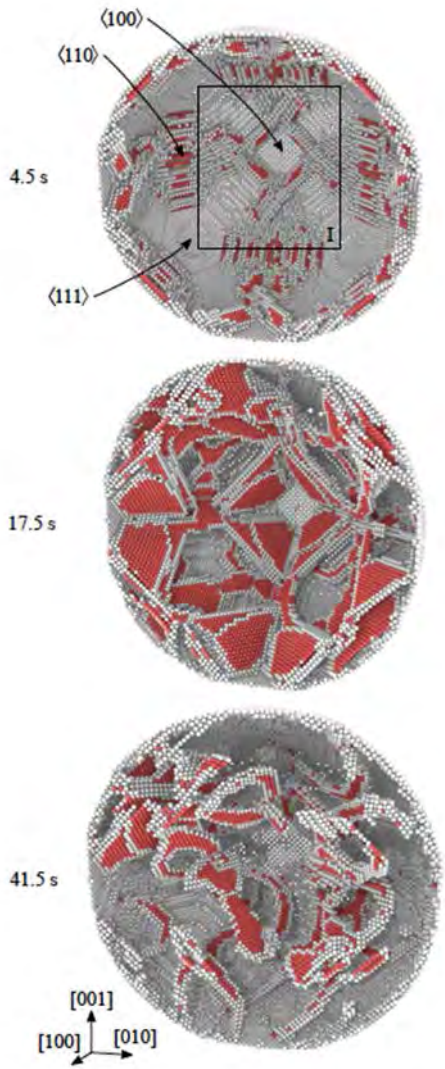

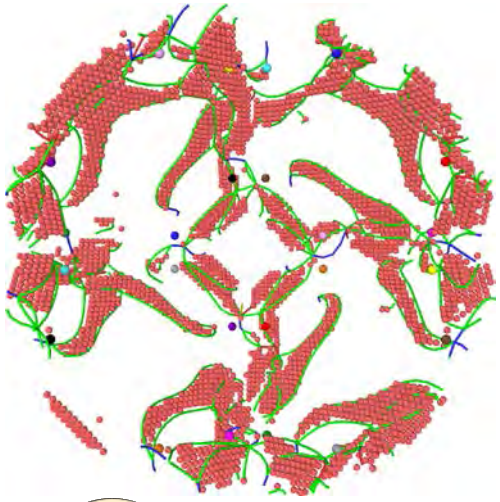

(100) plane

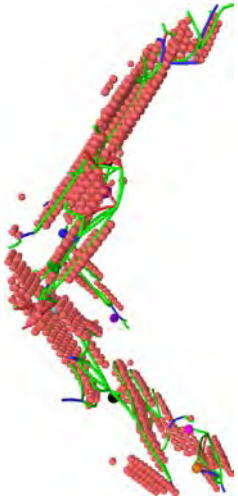

(111) direction

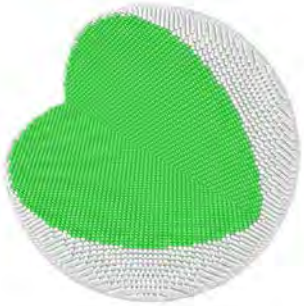

X. Sun, M. P. Ariza, M. Ortiz, K. G. Wang, *JMPS* (submitted).

Michael Ortiz
MPIE 2018

Work in progress: Mg–Al alloys

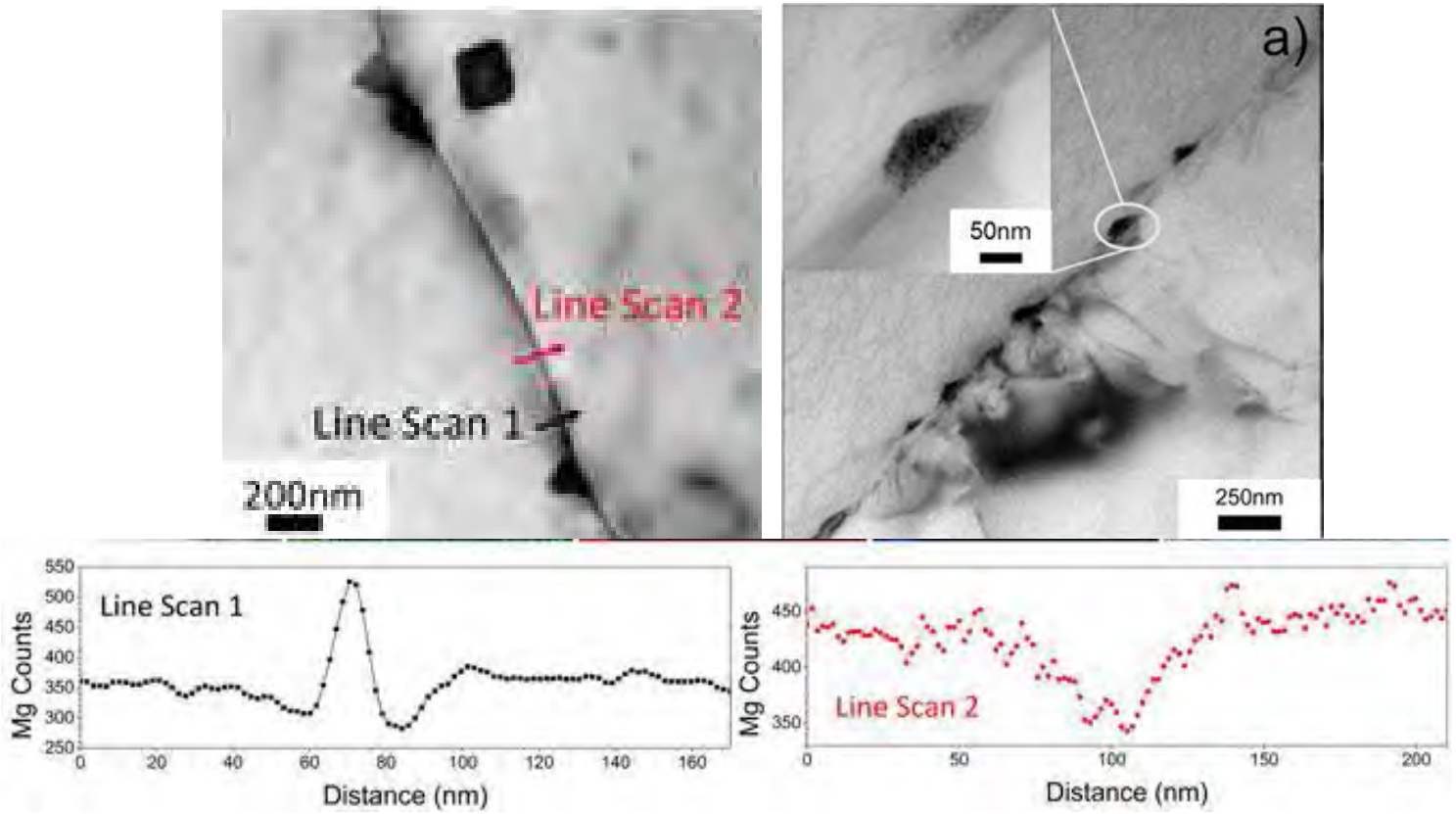

- Al-Mg 5xxxx series alloys
- Sensitization due to GBs
- Formation of β phase (Mg_2Al_3)
- Stress corrosion cracking

Time scale: ~ days!
Not accessible to MD

R. Zhang *et al.*, *Scientific Reports*, 7 (2017) 2961

DMD validation – Surface segregation

Al-4%Mg alloy at 600K

(100) surface **(110) surface** **(111) surface**

$D(T=600K) = 5.4914^{-16} m^2/s$

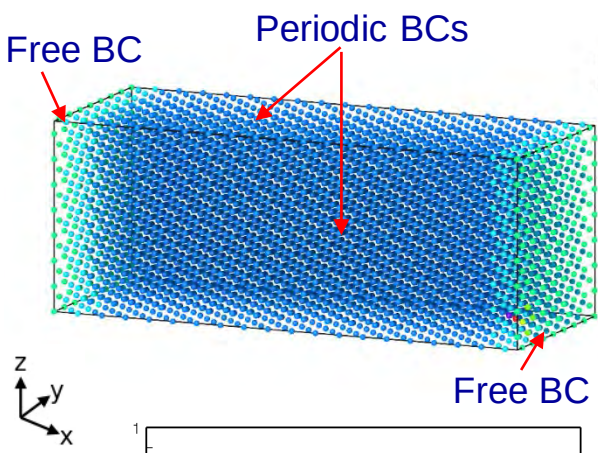

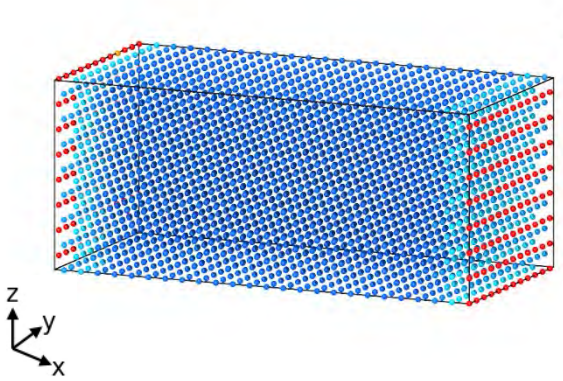

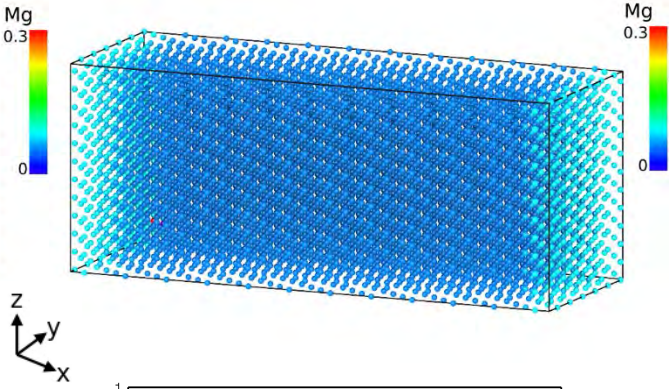

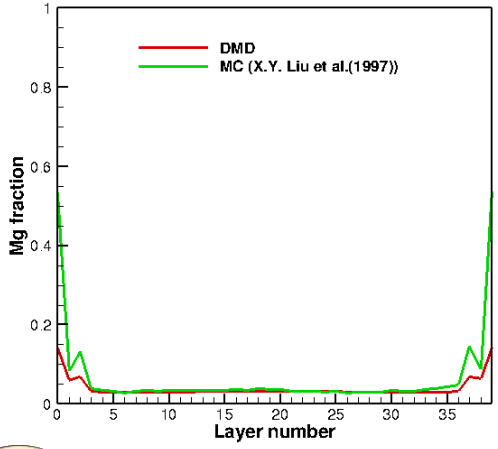

After 71 ms

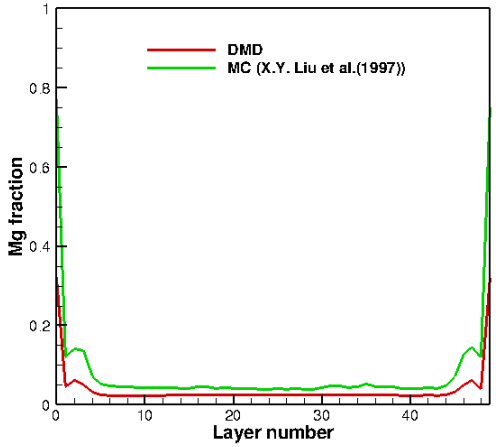

After 82 ms

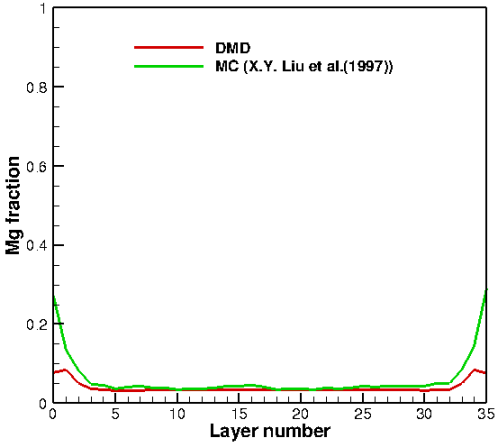

After 142 ms

E. Dontsova, *et al.*, *Phys. Rev. B*, **90** (2014) 174102

Michael Ortiz
MPIE 2018

DMD validation – GB segregation

Al-4%Mg alloy at 600K

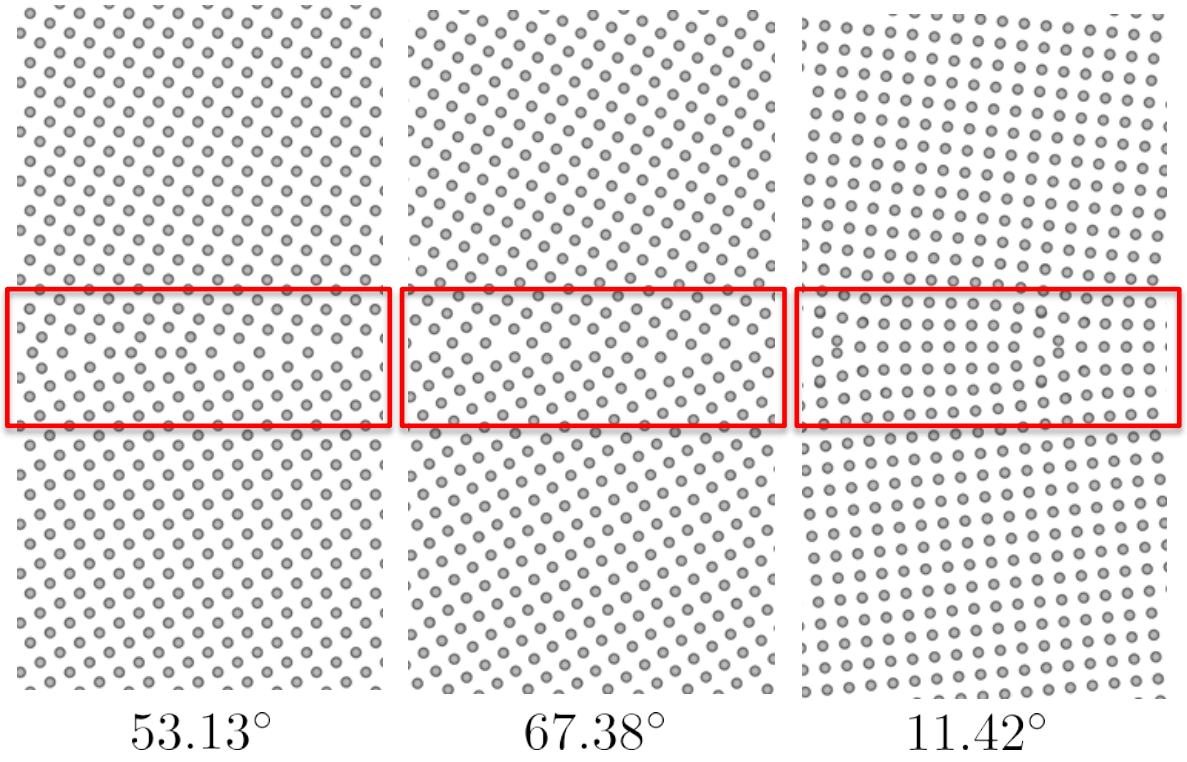

Symmetric grain boundary energies

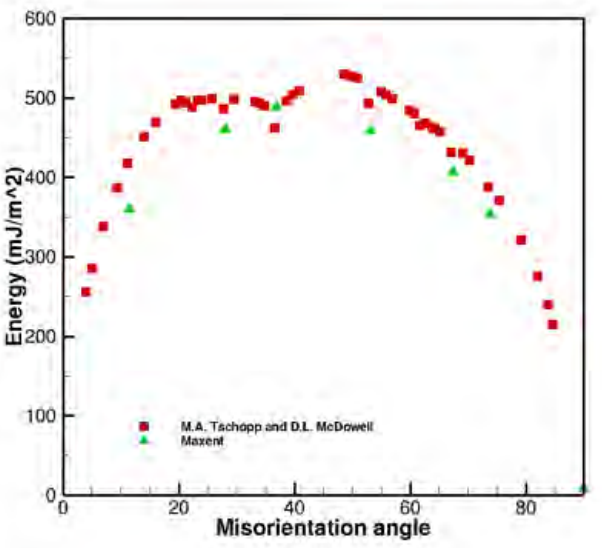

Michael Ortiz
MPIE 2018

DMD validation – GB segregation

Al-4%Mg alloy at 300K

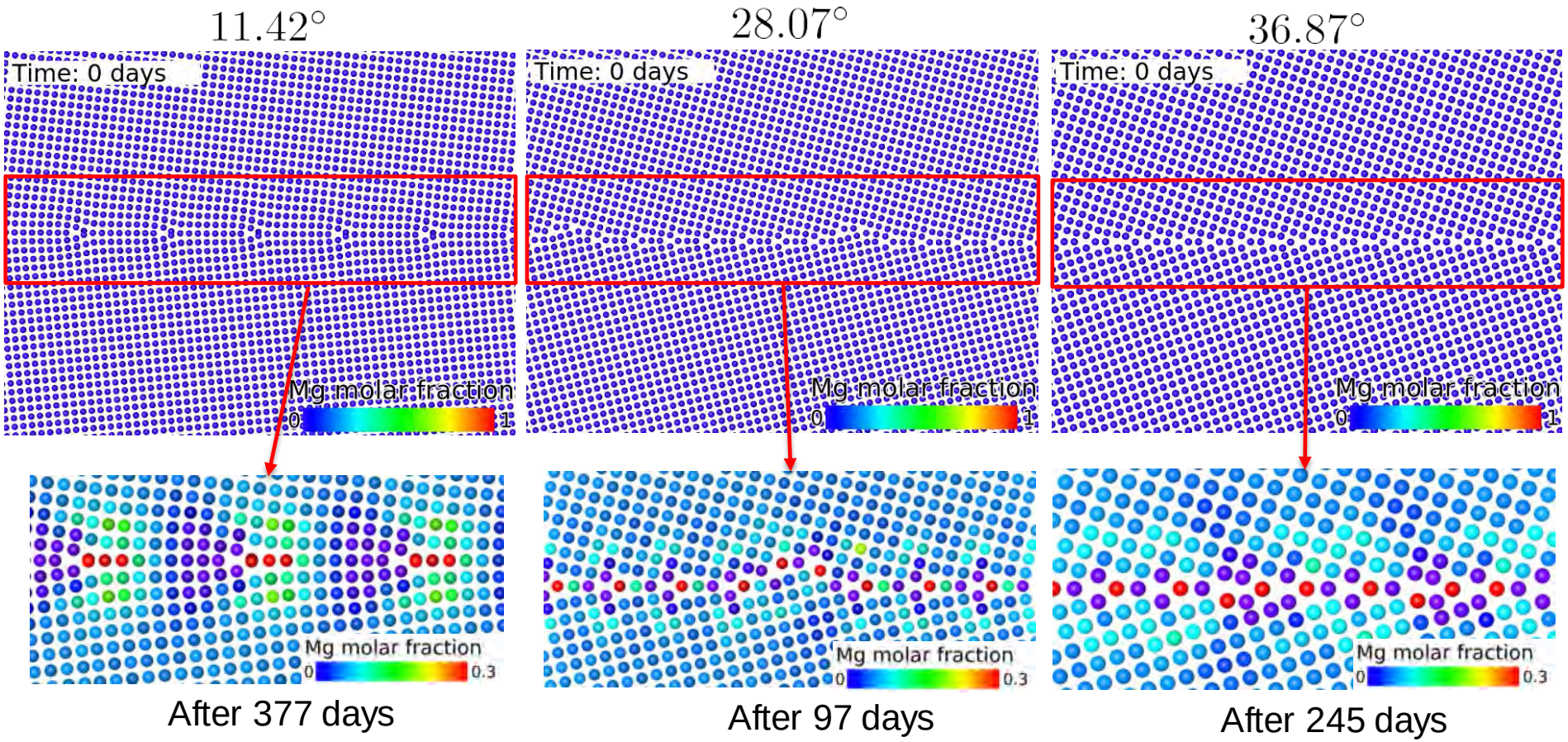

Z. Li, *et al.*, *Scientific Reports*, **6** (2016) 29973.

DMD validation – GB segregation

Al-4%Mg alloy at 300K

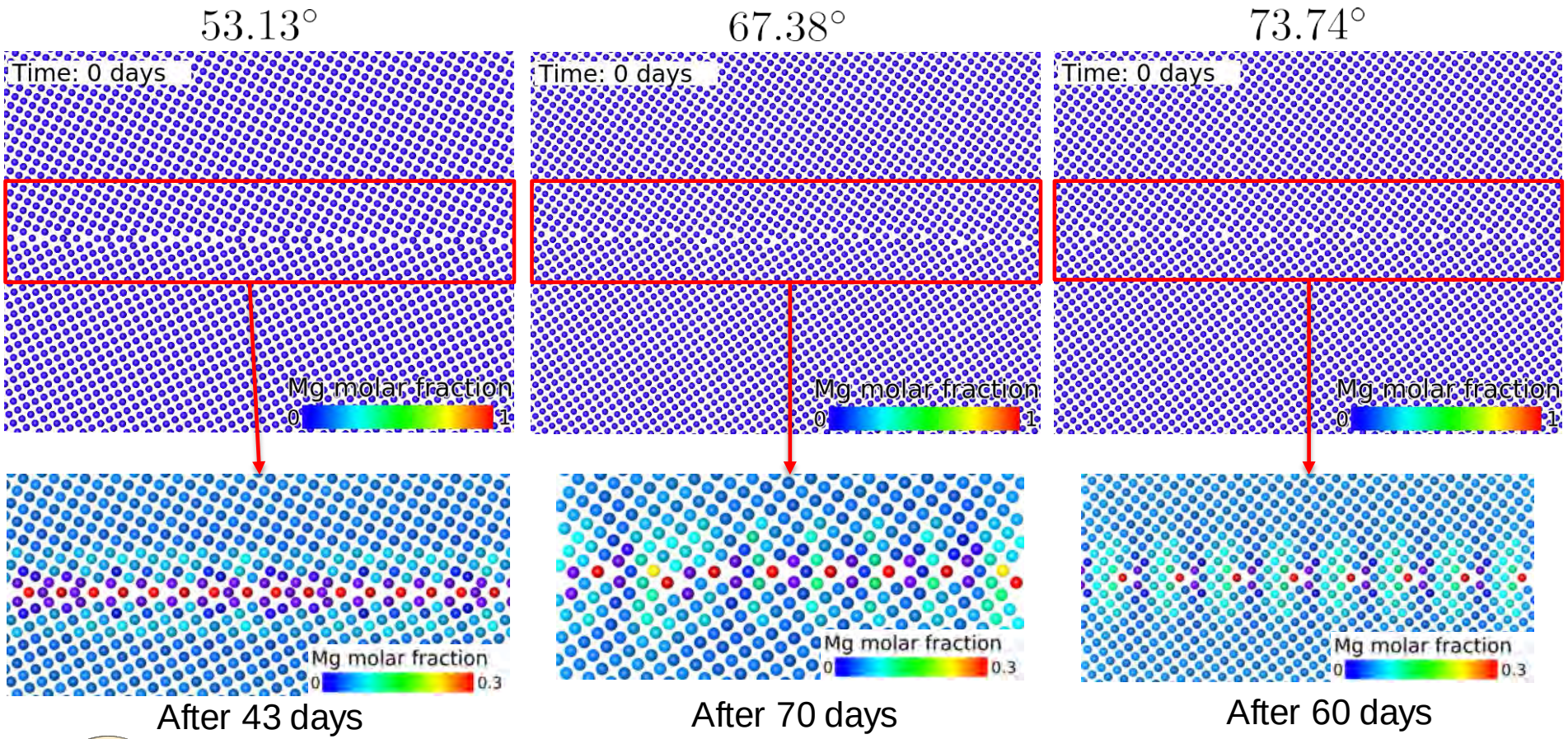

Z. Li, *et al.*, *Scientific Reports*, **6** (2016) 29973.

Michael Ortiz
MPIE 2018

DMD validation – GB segregation

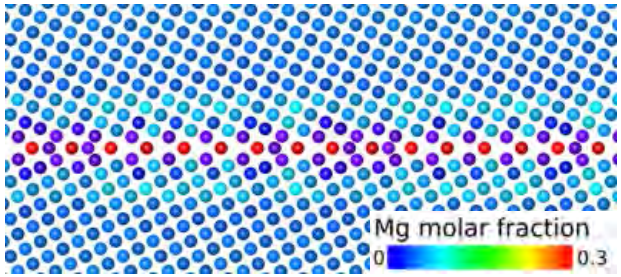

After 43 days

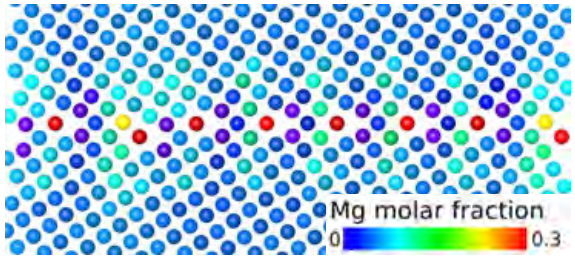

After 70 days

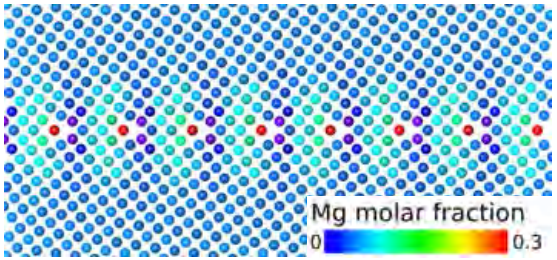

After 60 days

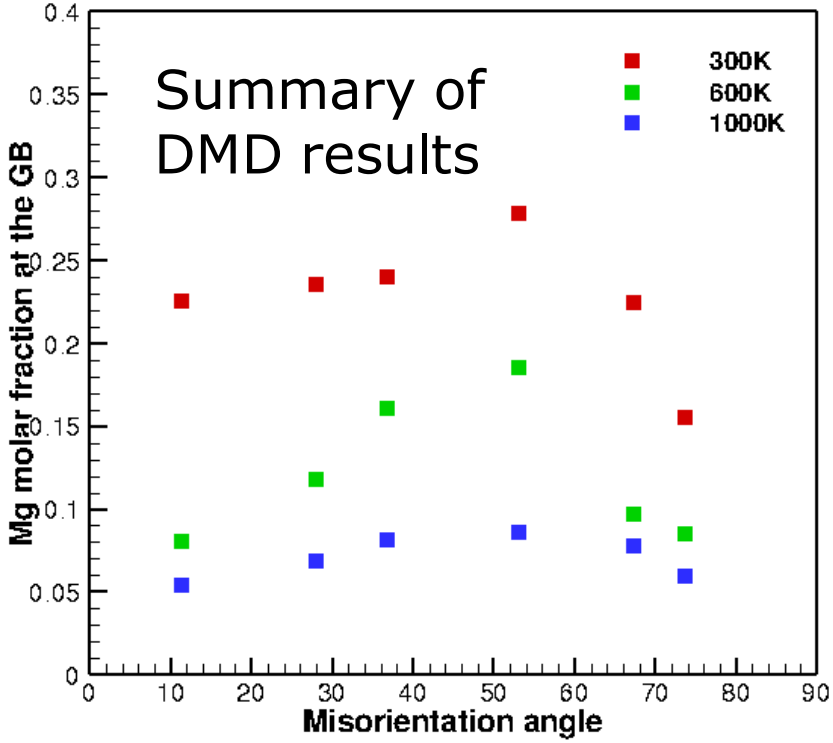

- Mg segregation to Al GBs takes place on time scale of days or months.
- Mg segregation to Al GBs depends on misorientation angle
- Mg segregation to Al GBs depends on temperature.
- An increase in temperature reduces segregation

DMD validation – GB segregation

Al-4%Mg alloy at 300K
Dissolution of Mg precipitate

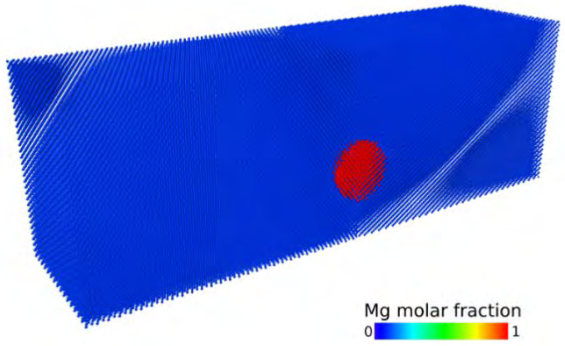

After 0 days

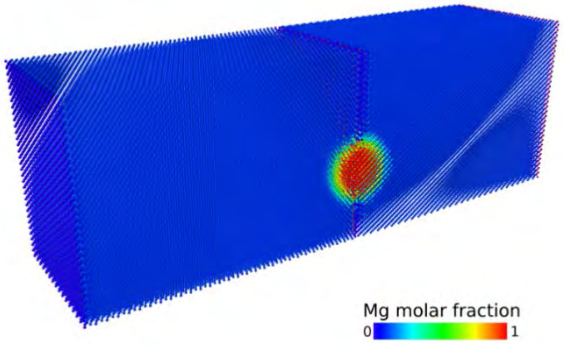

After 1 days

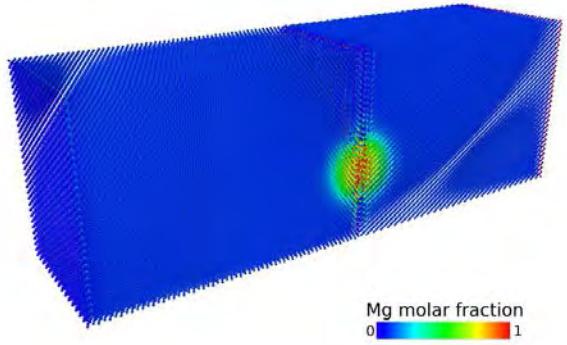

After 2 days

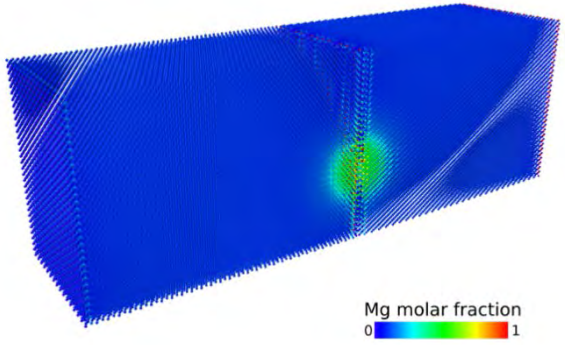

After 12 days

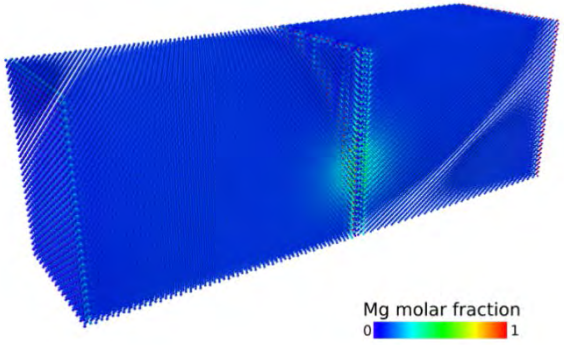

After 20 days

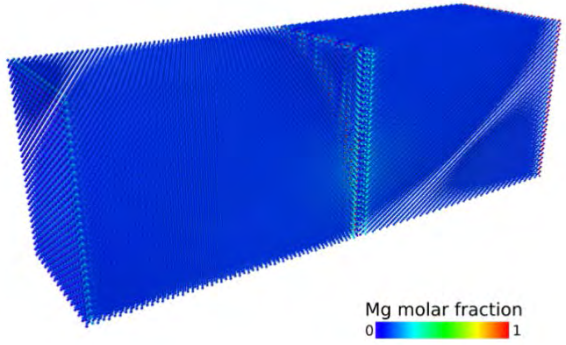

After 69 days

Z. Li, *et al.*, *Scientific Reports*, **6** (2016) 29973.

Al-4%Mg Polyxals – Mechanical testing

After 84 hours

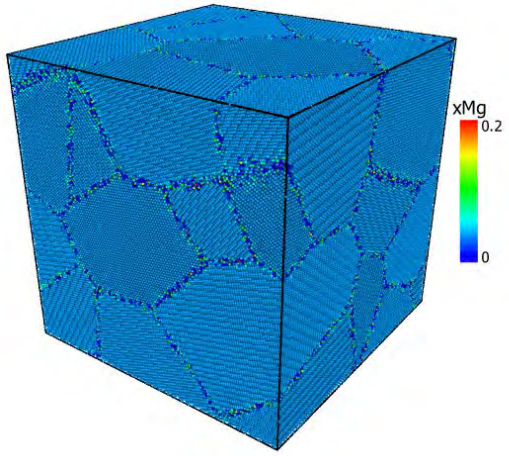

Uniaxial test - strain rate: 1e10 1/sec

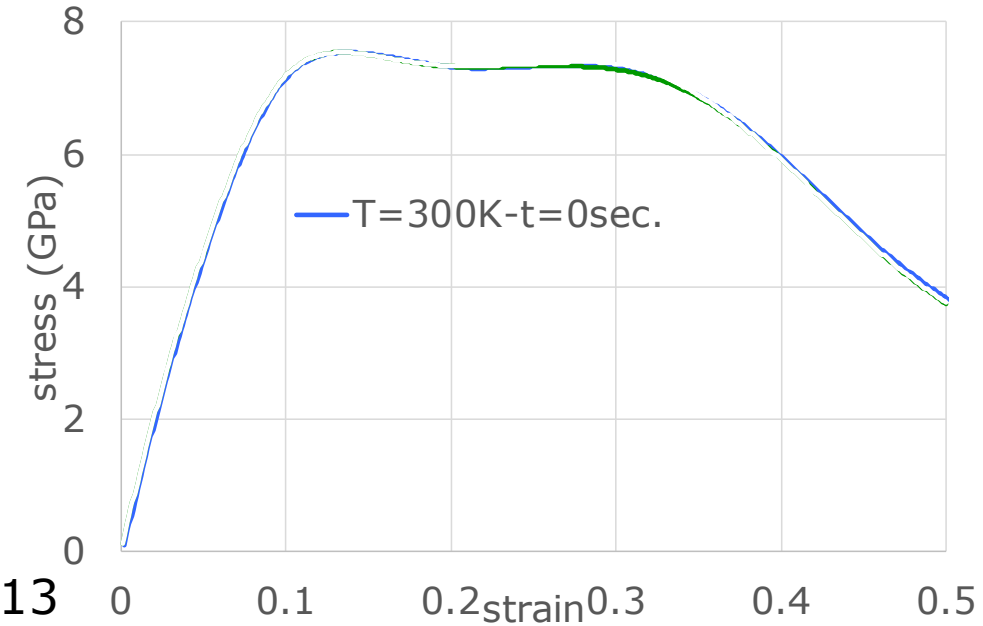

$D(T=300K) = 3.3364^{-26}\ m^2/s$
Hopping frequency (1/s) = 1.0e13
Barrier energy (eV) = 1.1542

Frequency

$\varepsilon = 0.15$

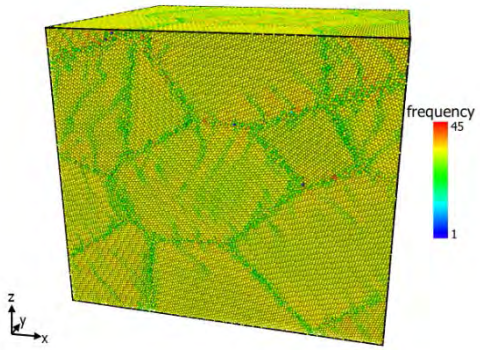

Dislocation analysis

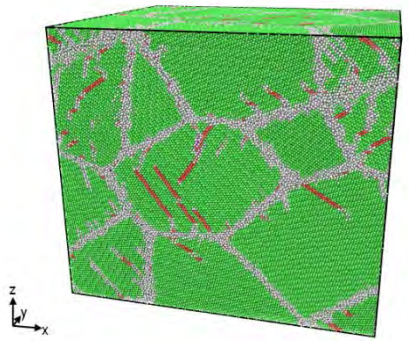

Color	Structure	Count	Fraction
	Other	426934	19.7%
	FCC	1675814	77.4%
	HCP	61698	2.9%
	BCC	0	0.0%
	Cubic diamond	0	0.0%
	Hexagonal diamond	0	0.0%

Michael Ortiz
MPIE 2018

Concluding remarks

- *Diffusive Molecular Dynamics* (DMD) provides a useful paradigm for describing slow/long term diffusion/transport phenomena with atomistic realism
- Non-equilibrium thermodynamics without all the thermal vibrations; mass transport without all the hops; atomistics without all the atoms…
- Work in progress: Microstructure evolution in alloys (work in collaboration with SINTEF/ Norway, NTNU, HZG…)

Michael Ortiz
MPIE 2018